To the Graduate Council:

I am submitting herewith a dissertation written by Peter Ping-yi Tsai entitled "ELECTRICAL MEASUREMENTS APPLIED TO ANISOTROPIC MECHANICS OF MELT BLOWN THIN WEBS." I have examined the final copy of this dissertation for form and content and recommend that it be accepted in partial fulfillment of the requirements for the degree of Doctor of Philosophy, with a major in Human Ecology.

Randall R. Bresee, Major Professor

We have read this dissertation
and recommend its acceptance:

Accepted for the Council:

Vice Provost
and Dean of The Graduate School

ELECTRICAL MEASUREMENTS APPLIED TO
ANISOTROPIC MECHANICS OF MELT BLOWN THIN WEBS

A Dissertation

Presented for the

Doctor of Philosophy

Degree

The University of Tennessee, Knoxville

Peter Ping-yi Tsai

December 1990

ACKNOWLEDGEMENT

Financial support from INDA through the 1988-89 Academic Research Grant and from the University of Tennessee Center for Materials Processing are greatly appreciated. Exxon Chemical Corporation is gratefully acknowledged for providing the melt blown pilot plant and technical support to the University.

ABSTRACT

Elastic constants of fibrous materials can not be easily determined experimentally using classical anisotropic theory of elasticity. Instead, constants are more easily computed theoretically using fiber-web theory since the only parameter appearing in constant-determination functions is the fiber orientation distribution function. However, no technique currently exists to measure this parameter conveniently and accurately.

This Dissertation involves developing a method to measure the fiber orientation distribution. The method is based on electrical measurements. The fiber orientation distribution determined in this manner is especially suitable for use in elastic constant-determination functions since it takes into account the variable fiber cross-sectional area usually found in actual webs.

Typical textile materials exhibit high electrical resistance and an instrument was designed to measure the low electric current conducted through webs. A theory based on the electrical field applied by the instrument also was developed to convert measured electrical currents to the fiber orientation distribution. Results were compared with both tensile testing and the actual distribution determined by counting fibers while webs were viewed with an optical

microscope. Excellent agreements were found.

TABLE OF CONTENTS

1. INTRODUCTION 1

2. REVIEW OF TECHNIQUES FOR DETERMINING THE FIBER ORIENTATION DISTRIBUTION 3

2.1 Microscope Counting 3

2.2 Modified Microscope Technique 4

2.3 Light Reflection and Refraction Intensity . . 4

2.4 Infrared Absorption 5

2.5 Zero-span Tensile Testing 7

2.6 X-ray Diffraction 8

2.7 Laser-beam Diffraction 9

2.8 Ultrasonic Wave Propagation 10

3. ANISOTROPIC MECHANICS 11

3.1 Theory of Elasticity 11

3.1.1 Anisotropic Webs 12

3.1.2 Orthotropic Webs 14

3.1.3 Isotropic Webs 16

3.2 Fiber-web Theory 17

4. FIBER ORIENTATION DISTRIBUTION BY ELECTRIC MEASUREMENTS 28

4.1 Theory 28

4.1.1 The General Anisotropic Case 35

4.1.2 The Orthotropic Case 36

4.1.3 The Isotropic Case 38

4.2 Instrumentation 39

5. EXPERIMENTAL 52

6. RESULTS AND DISCUSSION 61

7. CONCLUSIONS AND COMMENTS 89

LIST OF REFERENCES 91

APPENDIX 95

VITA 112

LIST OF TABLES

Table 5.1 Processing conditions to make three different fiber-oriented webs. 54

Table 6.1 Fiber orientation distribution of three webs from electrical measurements. 65

Table 6.2 Fiber orientation distribution of highly oriented web from fiber counting. 66

Table 6.3 Normalized axial compliance constants of three webs computed from fiber-web theory using fiber orientation distributions obtained from electrical measurements. 68

Table 6.4 Normalized axial compliance constants from tensile testing and from counting fibers under microscope. 70

Table 6.5 Non-dimensional compliance constants* of low oriented web computed from fiber-web theory using the fiber orientation distribution obtained from electrical measurements. . . 75

Table 6.6 Non-dimensional stiffness constants* of low-oriented web computed from fiber-web theory using the fiber orientation distribution from electrical measurements. 76

Table 6.7 Non-dimensional compliance constants* of medium-oriented web computed from fiber-web theory using the fiber orientation distribution obtained from electrical measurements. . . 77

Table 6.8 Non-dimensional stiffness constants* of medium-oriented web computed from fiber-web theory using the fiber orientation distribution obtained from electrical measurements. . . 78

Table 6.9 Non-dimensional compliance constants* of highly-oriented web computed from fiber-web theory using the fiber orientation distribution obtained from electrical measurements. . . 79

Table 6.10 Non-dimensional stiffness constants* of highly-oriented web computed from fiber-web theory using the fiber orientation distribution obtained from electrical measurements. . . 80

Table 6.11 Non-dimensional compliance constants* of highly-oriented web computed from fiber-web theory using fiber orientation distribution obtained from counting fibers under microscope. . . 83

Table 6.12 Non-dimensional stiffness constants* of highly-oriented web computed from fiber-web theory using fiber orientation distribution obtained from counting fibers under microscope. . . 84

LIST OF FIGURES

Fig. 3.1 Web subjected to forces results in tension strain of fibers in θ-direction. 18

Fig. 3.2 Tension stress in y-direction caused tension strain of fibers in θ-direction. 25

Fig. 4.1 Chart demonstrating the superposition of global contribution matrix from local contribution factors. 37

Fig. 4.2 Variation of nylon resistance with temperature at 6% moisture content [25]. 40

Fig. 4.3 Variation of resistance with moisture content at 20^0C [25]. 41

Fig. 4.4 First generation instrument allowing variable sample length. 43

Fig. 4.5 Dependence of measured current on action of the humidifier and dehumidifier. 44

Fig. 4.6 Second generation instrument adding control of relative humidity in the chamber. 45

Fig. 4.7 Electrometer circuit for determining the fiber orientation distribution. 47

Fig. 4.8 Illustration of third generation instrument system that measures the currents of high-resistance materials. 48

Fig. 4.9 Inside of the chamber shows the saturated salt solution on the bottom and an Omega transmitter for measuring temperature and relative humidity. 50

Fig. 4.10 A close look at the sample holder. High voltage is supplied by the top brush and current is drawn by the bottom brush. 51

Fig. 5.1 Melt blown pilot line at the University of Tennessee. 53

Fig. 5.2 Photomicrograph of low-oriented web. 55

Fig. 5.3 Photomicrograph of medium-oriented web. . . 56

Fig. 5.4 Photomicrograph of highly-oriented web. . . 57

Fig. 5.5 A protractor template was used to cut twelve specimen in 15-degree direction intervals. . 58

Fig. 6.1 Currents measured at various temperature and relative humidity show the effect of measurement conditions. 62

Fig. 6.2 Current distribution from various measurement conditions. 64

Fig. 6.3 Comparison of normalized axial compliance constants of low-oriented web. 71

Fig. 6.4 Comparison of normalized axial compliance constants of medium-oriented web. 72

Fig. 6.5 Comparison of normalized axial compliance constants of highly-oriented web. 73

Fig. 6.6 Comparison of normalized axial compliance constants of highly-oriented web. 85

Fig. 6.7 Compliance constants of three webs based on electrical measurements. 87

LIST OF SYMBOLS

A	Web cross-sectional area; conductivity contribution matrix
A_f	Fiber cross-sectional area
C	Stiffness constant
C'	Stiffness constant in new axis
d	Distance in two parallel plates
E	Elastic modulus; electric field
E_f	Fiber elastic modulus
$f(\theta)$	Fiber orientation distribution function
G	Shear modulus
I	Electrical current
J	Electrical current density
L	Sample length
N	Total number of fibers in Web
n_k	Number of fibers in web k-direction
P_k	Probability of fiber occurrence in web k-direction
R	Electrical resistance
S	Compliance constant
S'	Compliance constant in new axis
X	Fiber orientation distribution vector

LIST OF SYMBOLS

(GREEK)

δ_{ij}	Kronecker delta
ϵ	strain
η, μ	Stress-strain coupling constants
ρ	Electrical conductivity in circuit theory
σ	Stress; electrical conductivity in field theory
τ	Shear stress
Φ	Potential function

CHAPTER 1

INTRODUCTION

There has been much interest in meltblown nonwoven webs during the last two decades. Web properties that have contributed to this interest include excellent filtration efficiency and barrier properties against bacteria. However, mechanical properties are generally thought to restrict the potential use of meltblown webs in many applications. Some physical properties of meltblown webs have been studied by Wadsworth et al. at the University of Tennessee [1,2]. However, anisotropic mechanical properties have received little study.

Backer et al. [3] and Cox [4] showed that elastic constants such as compliance constants, stiffness constants, and Poisson's ratios in webs such as paper and some nonwoven textiles depend on the fiber orientation distribution function. These constants are basic stress-strain coefficients so that, once they are known, the deformation of the material under various states of stress can be predicted. Knowledge of these constants allows most web mechanical properties to be understood better. The end result of this knowledge, of course, is the potential to improve web mechanical properties.

Elastic constants of fibrous materials can not be easily determined experimentally using classical anisotropic theory of elasticity. Instead, constants are more easily computed theoretically using fiber-web theory since the only parameter appearing in constant-determination functions is the fiber orientation distribution function. However, no technique currently exists to measure this parameter conveniently and accurately.

This Dissertation involves developing a method to measure the fiber orientation distribution. The method is based on electrical measurements. The fiber orientation distribution determined in this manner is especially suitable for use in elastic constant-determination functions since it takes into account the variable fiber cross-sectional area usually found in actual webs.

Typical textile materials exhibit high electrical resistance and an instrument was designed to measure the low electric current conducted through webs. A theory based on the electrical field applied by the instrument also was developed to convert measured electrical currents to the fiber orientation distribution. Results were compared with both tensile testing and the actual distribution determined by counting fibers while webs were viewed with an optical microscope. Excellent agreements were found.

CHAPTER 2

REVIEW OF TECHNIQUES FOR DETERMINING THE FIBER ORIENTATION DISTRIBUTION

Various techniques have been developed to obtain information about the fiber orientation distribution. They include microscope counting, modified microscope techniques, measurements of light reflection and refraction intensity, infrared absorption, zero-span tensile testing, x-ray diffraction, and laser-beam diffraction. Most of these were developed for papers.

2.1 Microscope Counting

The number of fibers aligned in different directions are counted while a web is viewed with a microscope. Although this is tedious and time-consuming, it is probably the most common technique in current use. Unfortunately, only fibers on the web surface can be counted so a bulk measure of fiber orientation is not obtained except for very thin webs. In addition, fiber diameter is ignored so only a number average orientation distribution is obtained. To reduce measurement tedium, sometimes a few dyed fibers are added and only these are counted. This saves time but reduces accuracy. Another problem with this technique is the uncertainty in assigning a direction to fibers since most do not lay straight in webs.

2.2 Modified Microscope Technique

The microscope technique has been modified and improved somewhat with the use of a computer. Fleischman [5] traced along fibers and then input their length and direction into a computer. The computer sums the total length in every defined direction so the fraction of total fiber length oriented in all directions is an indication of the fiber orientation distribution. Alternatively, Crosby et al. [6] divided fibers into segments and defined the segments in angles according to the prescribed coordinate. Segments in separate directions are summed to obtain the fiber orientation distribution. Neither Fleischman nor Crosby et al. considered fiber diameter; therefore, only number average distributions were obtained.

2.3 Light Reflection and Refraction Intensity

Orchard [7] applied the theory that when a fiber of circular cross-sectional shape is illuminated, the reflected and refracted light will form a cone of rays coaxial with the fibers and the cone semi-angle equals that between the fiber axis and the incident beam. In so far as this is true, fiber orientation distribution information can be obtained by intensity measurements from a photocell. The fiber orientation distribution was expressed as the following orientation coefficient,

$$coefficient = \frac{\max.\,photocell\,output}{\min.\,photocell\,output} - 1 \qquad (2.1)$$

When the coefficient equals 0, fibers in the web are said to be perfectly randomly distributed. No other information about the fiber orientation distribution was presented. Unfortunately, no theory was developed to relate light intensity to the number of fibers. Light diffraction and scattering were not considered. In addition, this technique may only be applied to loose and thin fiber webs.

2.4 Infrared Absorption

Boulay et al. [8,9,10] used a submillimeter wavelength absorption ratio as an indication of fiber orientation distribution, in which

$$anisotropy\ ratio = \frac{K_{md}}{K_{cd}} \qquad (2.2)$$

Where K_{md} and K_{cd} are absorption coefficients of polarized infrared light in machine and cross directions, respectively. Transmitted light intensity is the measured parameter and is related to absorption coefficients as follows:

$$T = \exp\{-(KX)\} \qquad (2.3)$$

where T = transmission coefficient, K = sample absorption coefficient, and X = sample basis weight.

Since moisture content influenced transmittance, equation (2.3) had to be modified as follows

$$T = \exp\{-(K_f X_f + K_w X_w)\} \qquad (2.4)$$

where K_f = fiber absorption coefficient, X_f = fiber basis weight, K_w = water absorption coefficient, and X_w = water basis weight.

Different anisotropy ratios were obtained when using different wavelengths but no technique was developed to control humidity and to relate the fiber number to submilimeter wavelength absorption. Submilimeter wavelengths occupy the far infrared region of the electromagnetic spectrum. Although this technique was developed for cellulose paper samples, limited infrared absorption could restrict application to other fibers.

The anisotropic ratio determined by this technique was compared with data obtained from zero-span tensile testing and agreement was satisfactory. However, data from zero-span testing and other methods do not compare satisfactorily. It must be concluded that the ratio of machine direction to cross direction as obtained by the infrared absorption is only a weak indication of the fiber orientation distribution.

2.5 Zero-span Tensile Testing

Kallmes [11] applied the following theory to obtain the fiber orientation distribution function in paper:

$$f(\theta) = \frac{1}{\pi} + e\cos 2\theta \qquad (2.5)$$

where $f(\theta)$ = fiber orientation distribution function, and

$$e = \frac{3}{2\pi}\,\frac{(1 + Z_{md}/Z_{cd})}{(1 - z_{md}/Z_{cd})} \qquad (2.6)$$

where Z_{md} = machine direction zero-span breaking length and Z_{cd} = cross direction zero-span breaking length. Unfortunately, the results did not compare satisfactorily with data from other techniques. The theory was obtained through personal communication and was unavailable in the public literature. A sound basis for this theory may not exist. We can see that when $Z_{md} = Z_{cd}$ (i.e. isotropic materials) a value of zero in the denominator results. In addition, it is obvious that the same Z_{md} and Z_{cd} values could yield different fiber orientation distribution functions. The fiber orientation distribution can predict all web elastic constants but elastic constants can't be determined by tensile testing alone. Consequently, one must question the validity of determining the fiber orientation distribution by only two tensile measurements, one in machine direction and the other in the cross direction.

2.6 X-ray Diffraction

Prud'homme, et al. [12] began with the assumption

$$N(\epsilon) = \frac{c}{c^2 \sin^2\epsilon + \cos^2\epsilon} \qquad (2.7)$$

where N(ϵ) is the fiber orientation distribution function and c is an experimentally determined orientation parameter. The x-ray diffraction intensity was then written as follows:

$$I(\Phi) = K \int_{\epsilon} N(\epsilon)\, D(\beta - \epsilon)\, d\epsilon \qquad (2.8)$$

where D(β) is the fibril angle distribution function of the sample which was independently determined by polarized optical microscopy.

The orientation function was obtained from the measured x-ray diffraction intensity after comparison to the theoretical intensity. Once D(β) was determined for selected papers, theoretical integrals were computed so a set of orientation parameters were predetermined. A theory was developed to relate the x-ray diffraction intensity to the fiber orientation distribution function. However, the fiber orientation distribution was assumed to have a specific functional form without giving the reason. In addition, the fibril angle distribution was directly determined by the birefrigence value without developing a theoretical relationship.

2.7 Laser-beam Diffraction

Rudström and Sjölin [13] analyzed laser beam diffraction patterns to determine the fiber orientation distribution. Their theory was based on the familiar two-dimensional Fourier transform [14]. In this technique, the diffracted electrical field amplitude, $E_f(r,s)$ is the integral of the amplitude transmittance function of the diffraction object, $t_0(x,y)$, as follows:

$$E_f(r,s) = A/j\lambda f \int_{-\infty}^{\infty}\!\!\int t_o(x,y) \exp[(-j2\pi/\lambda f)(xr+ys)]\, dx\, dy \tag{2.9}$$

The diffracted light intensity is the square of the electrical field amplitude, so

$$I_f(r,s) = A^2/\lambda^2 f^2 \left[\int_{-\infty}^{\infty}\!\!\int t_0(x,y) \exp[(-j2\pi/\lambda f)(xr+ys)]\, dxdy\right]^2 \tag{2.10}$$

Unfortunately, the authors didn't use these two equations to derive a relationship between fiber number and measured light intensity. Rather, they directly expressed the fiber number from the measured light diffraction intensity without considering optical phenomena such as scattering and refraction. Results from this technique were not compared to data from other techniques. A restriction of the technique is that it can be applied only to thin webs.

2.8 Ultrasonic Wave Propagation

Theory of vibration shows that the velocity, C, of a longitudinal wave propagating in the axial direction of an isotropic rod is equal to

$$C = \sqrt{E/\rho} \tag{2.11}$$

where E is the elastic modulus and ρ is the mass density of the rod. Thus, elastic moduli may possibly be determined by the wave velocity.

In a paper by Baum and Bornhoeft [15], the wave equation was written in terms of stiffness constants, C_{ij}'s, for orthotropic, two-dimensional materials as

$$C_{11}\frac{\partial^2 u_1}{\partial x^2} + C_{12}\frac{\partial^2 u_2}{\partial x \partial y} + C_{66}\left(\frac{\partial^2 u_2}{\partial x \partial y} + \frac{\partial^2 u_1}{\partial y^2}\right) = \rho\frac{\partial^2 u_1}{\partial t^2}$$

(2.12)

$$C_{66}\left(\frac{\partial^2 u_2}{\partial x^2} + \frac{\partial^2 u_1}{\partial x \partial y}\right) + C_{12}\frac{\partial^2 u_1}{\partial x \partial y} + C_{22}\frac{\partial^2 u_2}{\partial y^2} = \rho\frac{\partial^2 u_1}{\partial t^2}$$

where u_1 and u_2 are the longitudinal wave propagation velocity in x- and y- direction, respectively. Solving these two equations provides elastic moduli and Poisson's ratios. Consequently, this technique can be used to provide values of some elastic constants. However, it cannot be used to determine all of the constants or the fiber orientation distribution.

CHAPTER 3

ANISOTROPIC MECHANICS

The mechanics considered in this Dissertation consisted primarily of stress-strain relationships in the elastic region. Theory of elasticity [16,17,18] and anisotropic elasticity [19,20] treat these relationships in great detail. Elastic constants for the general case and three cases which occur most often for nonwoven webs (isotropic, orthotropic, and anisotropic) will be discussed only briefly here. Elastic constants can be obtained experimentally using theory of elasticity or they can be determined theoretically from fiber-web theory [4]. It will be shown that elastic constants are determined more conveniently from the latter.

3.1 Theory of Elasticity

The generalized Hooke's law relates the second-order stress tensor to the second-order strain tensor by the stiffness tensor, which is of the fourth order.

$$\boldsymbol{\sigma} = \boldsymbol{C} : \boldsymbol{\epsilon} \tag{3.1}$$

or

$$\sigma_{ij} = C_{ijkl} e_{kl} \tag{3.2}$$

where σ_{ij} denotes stresses, ϵ_{kl} denotes strains and C_{ijkl} denotes the stiffness constants. Although the number of constants totals 81, this number can be reduced for various conditions of symmetry.

3.1.1 Anisotropic webs

General anisotropic materials, a triclinic syngony, have no elements of symmetry. However, it can be shown that the stress tensor and strain tensor are each symmetric. If we assume the stiffness tensor also is symmetric, the number of the stiffness constants is reduced from 81 to 21 as follows:

$$\begin{bmatrix} C_{11} & C_{12} & C_{13} & C_{14} & C_{15} & C_{16} \\ \cdot & C_{22} & C_{23} & C_{24} & C_{25} & C_{26} \\ \cdot & \cdot & C_{33} & C_{34} & C_{35} & C_{36} \\ \cdot & \cdot & \cdot & C_{44} & C_{45} & C_{46} \\ \cdot & \cdot & \cdot & \cdot & C_{55} & C_{56} \\ \cdot & \cdot & \cdot & \cdot & \cdot & C_{66} \end{bmatrix} \tag{3.3}$$

Alternatively, generalized Hooke's law may be inverted to relate strain to stress by 81 compliance constants. Compliance constants usually are more experimentally accessible and stiffness constants may be obtained by inverting experimental measurements of compliance constants. In a way analogous to stiffness constants, the number of compliance constants may be reduced from 81 to 21 by symmetry considerations. If we express these 21 elastic constants in the engineering constant system, the compliance constants are

$$\begin{bmatrix} \frac{1}{E_{xx}} & -\frac{\nu_{yx}}{E_{xx}} & -\frac{\nu_{zx}}{E_{xx}} & \frac{\eta_{yz,x}}{E_{xx}} & \frac{\eta_{zx,x}}{E_{xx}} & \frac{\eta_{xy,x}}{E_{xx}} \\ -\frac{\nu_{xy}}{E_{yy}} & \frac{1}{E_{yy}} & -\frac{\nu_{zy}}{E_{yy}} & \frac{\eta_{yz,y}}{E_{yy}} & \frac{\eta_{zx,y}}{E_{yy}} & \frac{\eta_{xy,y}}{E_{yy}} \\ -\frac{\nu_{xz}}{E_{zz}} & -\frac{\nu_{yz}}{E_{zz}} & \frac{1}{E_{zz}} & \frac{\eta_{yz,z}}{E_{zz}} & \frac{\eta_{zx,z}}{E_{zz}} & \frac{\eta_{xy,z}}{E_{zz}} \\ \frac{\eta_{x,yz}}{G_{yz}} & \frac{\eta_{y,yz}}{G_{yz}} & \frac{\eta_{z,yz}}{G_{yz}} & \frac{1}{G_{yz}} & \frac{\mu_{zx,yz}}{G_{yz}} & \frac{\mu_{xy,yz}}{G_{yz}} \\ \frac{\eta_{x,zx}}{G_{xz}} & \frac{\eta_{y,zx}}{G_{xz}} & \frac{\eta_{z,zx}}{G_{xz}} & \frac{\mu_{yz,zx}}{G_{xz}} & \frac{1}{G_{xz}} & \frac{\mu_{xy,zx}}{G_{xz}} \\ \frac{\eta_{x,xy}}{G_{xy}} & \frac{\eta_{y,xy}}{G_{xy}} & \frac{\eta_{z,xy}}{G_{xy}} & \frac{\mu_{yz,xy}}{G_{xy}} & \frac{\mu_{zx,xy}}{G_{xy}} & \frac{1}{G_{xy}} \end{bmatrix} \tag{3.4}$$

where E = elastic modulus, ν = Poission's ratio, G = shear modulus, μ = the coefficients of Chentsov, and η = the coefficients of mutual influence.

The compliance constant matrix is symmetric since it is the inverse of a symmetric matrix, i.e

$$-\frac{\nu_{yx}}{E_{xx}} = -\frac{\nu_{xy}}{E_{xx}}, \; etc.$$

Coupling constants are coefficients describing the interactions between normal stresses and shear strains, between shear stresses and normal strains as well as between shear stresses and shear strains in different planes. Although important for describing mechanical behavior, coupling constants (μ,η) of fibrous materials are extremely difficult or even impossible to determine experimentally. Shear moduli (G) can't be experimentally determined with a tensile testing machine, the most commonly used machine for measuring the mechanical properties of nonwoven webs. Values of Poisson's ratio (ν) can not be experimentally determined conveniently with a tensile testing machine. Elastic moduli are more easily determined but one must assume that sample creep during testing can be neglected. The overall result of these considerations is that elastic constants are not conveniently obtained experimentally.

If webs are thin enough to be assumed two-dimensional, the number of the stiffness constants can be further reduced to six.

$$\begin{bmatrix} C_{11} & C_{12} & C_{16} \\ . & C_{22} & C_{26} \\ . & . & C_{66} \end{bmatrix} \tag{3.5}$$

The number of compliance constants may be similarly reduced to six.

3.1.2 Orthotropic webs

Orthotropic materials, a rhombic syngony, are a special case of anisotropic materials. Webs are geometrically orthotropic if fibers are oriented symmetrically with respect to two mutually perpendicular directions called the principal directions. Most nonwoven webs exhibit orthotropic properties to some degree because of the forward fiber flow and take-up action. The number of stiffness constants for three-dimensional orthotropic webs is reduced from 81 to 9 in their principal directions. The elastic constant matrix becomes

$$\begin{bmatrix} C_{11} & C_{12} & C_{13} & 0 & 0 & 0 \\ . & C_{22} & C_{23} & 0 & 0 & 0 \\ . & . & C_{33} & 0 & 0 & 0 \\ . & . & . & C_{44} & 0 & 0 \\ . & . & . & . & C_{55} & 0 \\ . & . & . & . & . & C_{66} \end{bmatrix} \qquad (3.6)$$

The coupling constants (μ,η) are no longer present. That is, the mutual interactions described previously disappears for orthotropic materials. For example, a square drawn on an orthotropic web becomes a rectangle after axial extension. Elastic moduli (E), Poisson's ratio (ν) and the shear moduli (G) are still included and continue to provide measurement difficulty as previously discussed. For two dimensional webs, the number of independent stiffness constants is further reduced to 4 and the matrix becomes

$$\begin{bmatrix} C_{11} & C_{12} & 0 \\ . & C_{22} & 0 \\ . & . & C_{66} \end{bmatrix} \qquad (3.7)$$

3.1.3 Isotropic Webs

Isotropic materials have an infinite number of axes of symmetry. The simplest webs are structurally isotropic and stress is related to strain by only two direction-independent constants, elastic modulus (E) and Poisson's ratio (ν). The relationship is

$$\underline{\sigma} = \frac{E}{1+\nu}\left(\underline{\epsilon} + \frac{\nu}{1-2\nu}\underline{I}\right) \tag{3.8}$$

or

$$\sigma_{ij} = \frac{E}{1+\nu}\left(\epsilon_{ij} + \frac{\nu}{1-2\nu}\delta_{ij}\,\epsilon_{kk}\right) \tag{3.9}$$

The elastic modulus and Poisson's ratio need to be experimentally determined and a web should be tested in several directions to prove the web exhibits isotropic properties.

In summary, we have learned that it is difficult to experimentally determine the elastic constants. Even the simple isotropic case requires the Poisson's ratio which is not conveniently accessible experimentally. What's more, an elastic constant matrix only describes stress-strain behavior in two or three directions. Values of the elastic constants in other directions must be either measured separately or obtained from the transformation equation

$$T'_{ijkl} = a_{im}a_{jn}a_{ko}a_{lp}\, T_{mnop} \qquad (3.10)$$

or

$$T_{ijkl} = a_{mi}a_{nj}a_{ok}a_{pl}\, T'_{mnop} \qquad (3.11)$$

For the general case, the transformation equation consists of 81 terms which leads to computational difficulty. In any case, stiffness constants usually are obtained by inverting experimental measurements of compliance constants.

3.2 Fiber-web Theory

In 1952, Cox [4] made three assumptions in deriving expressions of stiffness constants as a function of the fiber orientation distribution function. His three assumptions were:

1. Fibers are straight throughout the whole body of the material.
2. Flexural stiffness of a single fiber is negligible.
3. Fibers are bonded rigidly together.

Suppose that a thin web is subjected to forces in such a way that the stresses are resolved as illustrated in Figure 3.1. Then, Cox showed that the strain of fibers oriented in the θ direction is

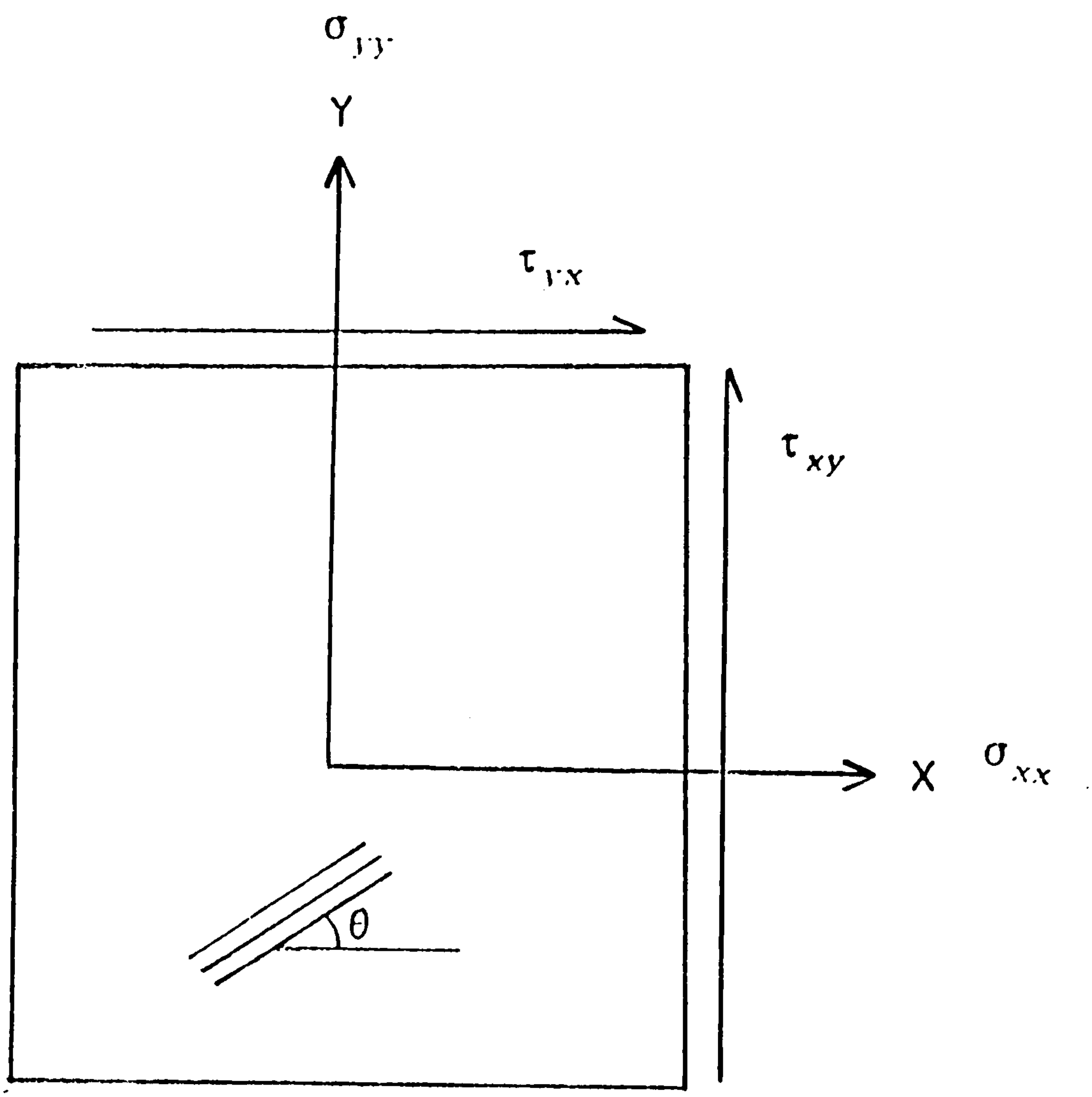

Fig. 3.1 Web subjected to forces results in tension strain of fibers in θ-direction.

$$e_f = e_x\cos^2\theta + e_y\sin^2\theta + 2e_{xy}\sin\theta\cos\theta \qquad (3.12)$$

where the subscript f refers to fibers and the subscripts x and y refer to web directions. Cox also showed the following:

$$\overset{\langle f\rangle}{\sigma}_x = \sigma_f\cos^2\theta$$

$$\overset{\langle f\rangle}{\sigma}_y = \sigma_f\sin^2\theta \qquad (3.13)$$

$$\overset{\langle f\rangle}{\tau}_{xy} = \sigma_f\sin\theta\cos\theta$$

where <f> denotes a single fiber and the shear stress σ_{xy} is denoted by τ_{xy}. Hooke's law applied to a single fiber yields

$$\sigma_f = E_f e_f \qquad (3.14)$$

Incorporating this into equations (3.12 & 3.13) yields

$$\sigma_x = E_f\int_{-\frac{\pi}{2}}^{\frac{\pi}{2}}(e_x\cos^2\theta + e_y\sin^2\theta + 2e_{xy}\sin\theta\cos\theta)\cos^2\theta f(\theta)d\theta$$

$$\sigma_y = E_f \int_{-\frac{\pi}{2}}^{\frac{\pi}{2}} (e_x \cos^2\theta + e_y \sin^2\theta + 2e_{xy} \sin\theta\cos\theta)\sin^2\theta f(\theta)\,d\theta \tag{3.15}$$

$$\tau_{xy} = E_f \int_{-\frac{\pi}{2}}^{\frac{\pi}{2}} (e_x \cos^2\theta + e_y \sin^2\theta + 2e_{xy} \sin\theta\cos\theta)\sin\theta\cos\theta f(\theta)\,d\theta$$

Thus, stiffness constants can be obtained by comparing with the stress and strain relationships and expressed as follows:

$$C_{11} = E_f \int_{-\frac{\pi}{2}}^{\frac{\pi}{2}} \cos^4\theta f(\theta)\,d\theta$$

$$C_{12} = E_f \int_{-\frac{\pi}{2}}^{\frac{\pi}{2}} \cos^2\theta \sin^2\theta f(\theta)\,d\theta = C_{21} = C_{66}$$

$$C_{22} = E_f \int_{-\frac{\pi}{2}}^{\frac{\pi}{2}} \sin^4\theta f(\theta)\,d\theta \tag{3.16}$$

$$C_{16} = E_f \int_{-\frac{\pi}{2}}^{\frac{\pi}{2}} \cos^3\theta \sin\theta f(\theta)\,d\theta = C_{61}$$

$$C_{26} = E_f \int_{-\frac{\pi}{2}}^{\frac{\pi}{2}} \sin^3\theta\cos\theta f(\theta)\,d\theta = C_{62}$$

Cox also expressed stiffness constants in terms of a Fourier series. Since the fiber orientation distribution function, f(θ), is a periodic function with a period of π, it was expressed in Fourier series as

$$f(\theta) = a_0 + \sum_{n=1}^{\infty} (a_n \cos 2n\theta + b_n \sin 2n\theta) \qquad (3.17)$$

where

$$a_0 = \frac{1}{\pi} \int_{-\frac{\pi}{2}}^{\frac{\pi}{2}} f(\theta)\,d\theta = \frac{1}{\pi}$$

$$a_n = \frac{2}{\pi} \int_{-\frac{\pi}{2}}^{\frac{\pi}{2}} f(\theta)\cos 2n\theta\,d\theta \qquad (3.18)$$

$$b_n = \frac{2}{\pi} \int_{-\frac{\pi}{2}}^{\frac{\pi}{2}} f(\theta)\sin 2n\theta\,d\theta$$

By neglecting the higher order terms (n>=3) and letting

$$\alpha_n = a_n x \pi = 2 \int_{-\frac{\pi}{2}}^{\frac{\pi}{2}} f(\theta) \cos 2n\theta \, d\theta$$

$$\beta_n = b_n x \pi = 2 \int_{-\frac{\pi}{2}}^{\frac{\pi}{2}} f(\theta) \sin 2n\theta \, d\theta \qquad (3.19)$$

One may write

$$\pi f(\theta) = 1 + \alpha_1 \cos 2\theta + \alpha_2 \cos 4\theta + \beta_1 \sin 2\theta + \beta_2 \sin 4\theta \qquad (3.20)$$

The functions $\cos^4\theta$, etc. in Eq. (3.16) may be written in the following forms:

$$\cos^4\theta = (\frac{1}{8})(3 + 4\cos 2\theta + \cos 4\theta)$$

$$\sin^4\theta = (\frac{1}{8})(3 - 4\cos 2\theta + \cos 4\theta)$$

$$\cos^2\theta \sin^2\theta = (\frac{1}{8})\,(1 - \cos 4\theta) \qquad (3.21)$$

$$\cos^3\theta \sin\theta = (\frac{1}{8})\,(2\sin 2\theta + \sin 4\theta)$$

$$\cos\theta\sin^3\theta = \left(\frac{1}{8}\right)(2\sin 2\theta - \sin 4\theta)$$

Substituting in C_{11}, etc, and performing integrations, Cox obtained

$$C_{11} = \frac{E_f}{16}(\alpha_2 + 4\alpha_1 + 6)$$

$$C_{12} = \frac{E_f}{16}(2 - \alpha_2) = C_{21} = C_{66}$$

$$C_{22} = \frac{E_f}{16}(\alpha_2 - 4\alpha_1 + 6) \qquad (3.22)$$

$$C_{16} = \frac{E_f}{16}(2\beta_1 + \beta_2) = C_{61}$$

$$C_{26} = \frac{E_f}{16}(2\beta_1 - \beta_2) = C_{62}$$

Strains generally must be written in terms of stress to determine the constants experimentally. Consequently, the stiffness constant matrix is inverted and written in the following forms to obtain elements of the compliance matrix:

$$S_{11} = [(2 - \alpha_2)(6 - 4\alpha_1 + \alpha_2) - (2\beta_1 - \beta_2)^2] / \Delta$$

$$
\begin{aligned}
S_{11} &= [(2 - \alpha_2)(6 - 4\alpha_1 + \alpha_2) - (2\beta_1 + \beta_2)^2] \,/\, \Delta \\
S_{12} &= -[(2 - \alpha_2)^2 - 4\beta_1^{\,2} + \beta_2^{\,2}] \,/\, \Delta \\
S_{16} &= -4[(2 - 2\alpha_1 + \alpha_2)\beta_1 + (2 - \alpha_1)\beta_2] \,/\, \Delta \\
S_{26} &= -4[(2 + 2\alpha_1 + \alpha_2)\beta_1 - (2 + \alpha_1)\beta_2] \,/\, \Delta \\
S_{66} &= 16(2 + \alpha_2 - \alpha_1^{\,2}) \,/\, \Delta
\end{aligned}
\tag{3.23}
$$

where

$$\Delta = E_f[(2 + \alpha_2 - \alpha_1^{\,2})(2 - \alpha_2 - \beta_1^{\,2}) - (\alpha_1\beta_1 - \beta_2)^2]$$

Like stiffness constants, compliance constants are expressed in terms of α's and β's which are each a function of the fiber orientation distribution function. Thus, every elastic constant is determined by the fiber orientation distribution function.

Baker, et al. [3] made assumptions similar to Cox and derived expressions for two elastic constants - the elastic modulus and Poisson's ratio - as a function of the fiber orientation function for nonwoven webs. He considered stress applied to a web in the y-direction as shown in Figure 3.2 so the strain of fibers at an angle θ to the y-direction is

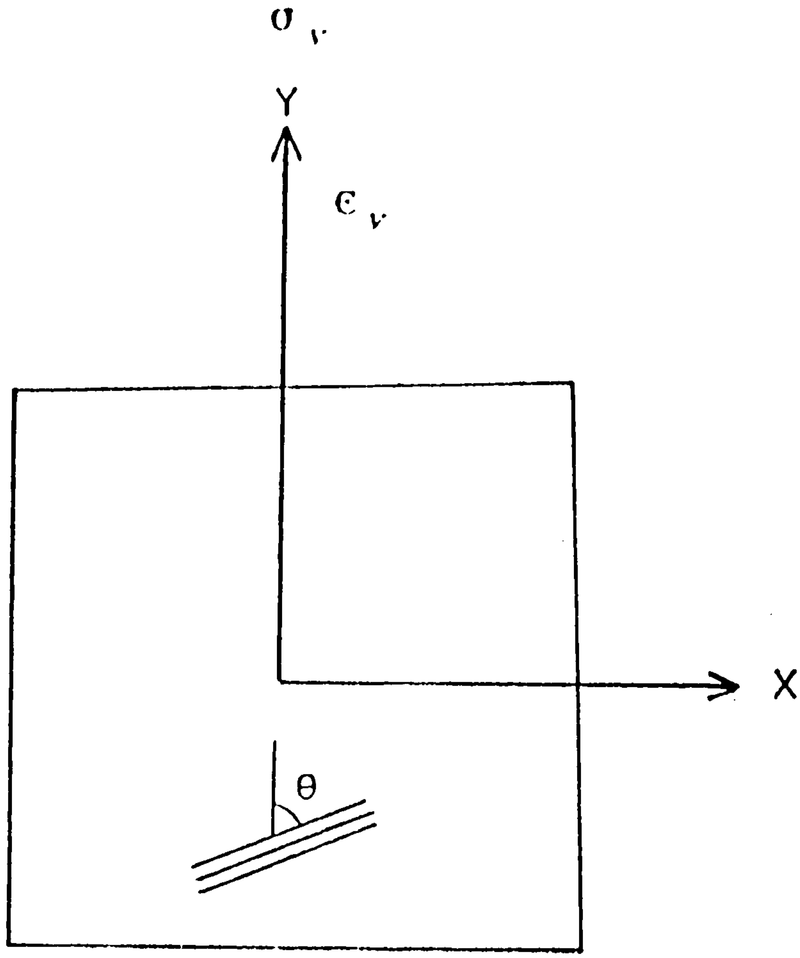

Fig. 3.2 Tension stress in y-direction caused tension strain of fibers in θ-direction.

$$\epsilon_f = \epsilon_y(\cos^2\theta - \nu_{xy}\sin^2\theta) \tag{3.24}$$

where ϵ_f denotes fiber strain, ϵ_y denotes web strain, and ν_{xy} denotes the web Poisson's ratio. The stress on individual fibers will be

$$\sigma_f = E_f\epsilon_f \tag{3.25}$$

where σ_f denotes fiber stress, E_f denotes fiber modulus and ϵ_f denotes fiber strain. Web stress in the y-direction exerted by the stress σ_f is

$$\sigma_y^{\langle f \rangle} = \sigma_f\cos^2\theta \tag{3.26}$$

Consequently, web stress in the y-direction can be represented by

$$\sigma_y = E_f\epsilon_y\int_{-\frac{\pi}{2}}^{\frac{\pi}{2}}[\cos^2\theta - \nu_{xy}\sin^2\theta]\cos^2\theta f(\theta)d\theta \tag{3.27}$$

where $f(\theta)$ is the fiber orientation distribution function. The stress in the web in the x-direction can be determined similarly and is

$$\sigma_x = E_f\epsilon_y\int_{-\frac{\pi}{2}}^{\frac{\pi}{2}}[\cos^2\theta - \nu_{xy}\sin^2\theta]\sin^2\theta f(\theta)d\theta \tag{3.28}$$

Since $\sigma_x = 0$ in the situation depicted in Figure 3.2, an expression for the web Poisson's ratio is obtained

$$\nu_{xy} = \frac{\int_{-\frac{\pi}{2}}^{\frac{\pi}{2}} \cos^2\theta \sin^2\theta f(\theta)\, d\theta}{\int_{-\frac{\pi}{2}}^{\frac{\pi}{2}} \sin^4\theta f(\theta)\, d\theta} \qquad (3.29)$$

Using the above equation, an expression for the web elastic modulus is obtained

$$E_y = E_f \int_{-\frac{\pi}{2}}^{\frac{\pi}{2}} \left[\cos^2\theta - \frac{\int_{-\frac{\pi}{2}}^{\frac{\pi}{2}} \sin^2\theta \cos^2\theta f(\theta)\, d\theta}{\int_{-\frac{\pi}{2}}^{\frac{\pi}{2}} \sin^4\theta f(\theta)\, d\theta} \sin^2\theta\right] \cos^2\theta f(\theta)\, d\theta \qquad (3.30)$$

Equation (3.29) shows that the web Poisson's ratio, ν_{xy}, is only a function of the fiber orientation distribution function. Equation (3.30) shows that the web modulus is determined by the fiber modulus and fiber orientation distribution function.

CHAPTER 4

FIBER ORIENTATION DISTRIBUTION BY ELECTRICAL MEASUREMENTS

In Chapter 3 we learned that each elastic constant for a nonwoven web is a function of the fiber orientation distribution function. In Chapter 2 we reviewed techniques that have been developed to provide information about the fiber orientation distribution. We recognized that none of these techniques determine the whole fiber orientation Distribution conveniently and adequately. In this dissertation, a theory was developed and an instrument was designed to determine the whole fiber orientation distribution conveniently from measured electric currents.

4.1 Theory

In basic physics [21], we learned that the electrical resistance of a material, R, is proportional to its length, L, and inversely proportional to its cross-sectional area, A, or

$$R = \rho \frac{L}{A} \tag{4.1}$$

where the proportionality constant, ρ, is a material property called resistivity.

Another well-known expression from basic physics relating resistance to current, I, and voltage, V, is

$$I=\frac{V}{R} \tag{4.2}$$

which is Ohm's law in practical form.

If fibers in a web are assumed to be straight and if the bonding points between fibers are assumed to be weak so that electrical resistance at the bonded points can be assumed to be infinite, fibers aligned in directions other than that being measured will not contribute to current in the measured direction. Equations (4.1) and (4.2) then can be combined to provide current in the k direction, I_k from n_k fibers of cross-sectional area, A_f, in a web of length, L, to obtain Equation (4.3).

$$I_k=\left(\frac{VA_f}{\rho L}\right) n_k \tag{4.3}$$

In this expression, the fiber cross-sectional area is assumed to be constant so the measured current is a function only of the number of fibers oriented in the measured direction.

Unfortunately, the fiber cross-sectional area in many materials is quite variable and Equation (4.3) must be rewritten so that measured current is a function of both the number and cross-sectional area of fibers oriented in the measured direction.

$$I_k = \sum\left(\frac{V}{\rho L}\right) A_k = \left(\frac{V}{\rho L}\right) \sum A_k \tag{4.4}$$

where A_k is the fiber cross-sectional area oriented in the k-direction. For either case, the number of fibers in some direction or the probability of the fiber distribution can be obtained from measured currents. The case of constant fiber cross-sectional area leads to

$$P_k = \frac{I_k}{\sum_{i=1}^{M} I_i} = \frac{n_k}{N} \tag{4.5}$$

where M is the number of web measurements, n_k is the number of fibers oriented in the k-direction, and N is the total number of fibers in the web. The case of variable fiber cross-sectional area leads to

$$P_k = \frac{I_k}{\sum_{i=1}^{M} I_i} = \frac{\sum A_k}{\sum_{\pi} A_i} \tag{4.6}$$

where π is a period, that is to sum the fiber cross-sectional area in every direction for a period. The fiber orientation distribution measured by electrical currents takes into account the fiber cross-sectional area.

In our experimental measurements, however, we learned that measured current was not a function of fiber orientation distribution as expressed in Equations (4.5) and (4.6) because fibers in many nonwoven webs are firmly bonded and the contribution current from fibers oriented in all directions to current in the measured direction must be considered. One assumption that may be adopted is to consider the electrical conductivity of bonded points to be identical to that of the fibers. Then, one may consider a fibrous web to be a combination of resistors in an electrical circuit. The measured current in any one direction becomes the result of conductance along fibers in every direction and a web may be modeled by circuit theory. Unfortunately, fibers are arranged in rather complicated ways in most nonwoven materials and no technique using electrical circuit theory exists for obtaining an equivalent resistance that would subsequently lead to the fiber orientation distribution.

Another possible approach involves restating Ohm's law somewhat differently than in Equation (4.2). Using electric field theory, Ohm's law in point form can be restated so current density, J, is related to electric field, E, by the conductivity constant, σ, for isotropic materials [22].

$$\underline{J} = \sigma \underline{E} \tag{4.7}$$

For the general anisotropic case, conductivity is not constant and must be replaced with a tensor of the second order. Current and electric field then are related as follows [23]:

$$\underset{\sim}{J} = \underset{\approx}{\sigma} : \underset{\sim}{E} \tag{4.8}$$

Elements of the conductivity tensor must be known to utilize this relationship. If α represents any arbitrary web direction of interest, fibers aligned in the direction β away from α contribute to conductivity in the α direction by the factor $\cos^2\beta$. Then, web conductivity in the α direction can be expressed as

$$\sigma_\alpha = N\,\sigma_f \int_\alpha^{\alpha+\pi} \cos^2(\theta-\alpha)\, f(\theta)\, d\theta \tag{4.9}$$

or equivalently,

$$\sigma_\alpha = N\,\sigma_f \int_0^{\pi} \cos^2(\theta-\alpha)\, f(\theta)\, d\theta \tag{4.10}$$

where N is the total number of fibers, σ_f is the fiber conductivity which was assumed to be constant, and $f(\theta)$ is the fiber orientation distribution function, in which

$$\int_\pi f(\theta)\, d\theta = 1 \tag{4.11}$$

Writing the current density tensor equation in its component form yields

$$\begin{aligned} J_1 &= \sigma_{11}E_1 + \sigma_{12}E_2 + \sigma_{13}E_3 \\ J_2 &= \sigma_{21}E_1 + \sigma_{22}E_2 + \sigma_{23}E_3 \\ J_3 &= \sigma_{31}E_1 + \sigma_{32}E_2 + \sigma_{33}E_3 \end{aligned} \tag{4.12}$$

A unidirectional electric field can be obtained by using two parallel plates of infinite length as the sample holder. Electric field is an exact differential so there exists a potential function Φ such that

$$\vec{E}(r) = -\nabla\Phi(r) \tag{4.13}$$

and the electric field between the two infinite parallel plates is

$$E = \frac{\Phi_{ab}}{d} = \frac{V}{d} \tag{4.14}$$

where V is the supplied voltage and d is the distance between the plates.

In fact, the sample holder configuration can not be two infinite plates. In addition, the sample will also distort the uniform electric field between the parallel plates. However, most of the electric field distortion and the fringing effect caused by finite sample holders will be canceled when measured currents are converted to current distribution.

Since the electric field is unidirectional, the electric field in the directions of the other two coordinate axes will disappear. By combining Equations (4.10) and (4.12) and integrating over area, s, we have

$$I_\alpha = \int_s \underset{\sim}{J} \cdot \underset{\sim}{ds}$$

$$I_\alpha = \sigma_f N A_f \frac{V}{d} \int_0^\pi \cos^2(\theta-\alpha) f(\theta) d\theta \tag{4.15}$$

$$I_\alpha = K \int_0^\pi \cos^2\theta f(\theta) d\theta$$

where K is a constant. Changing to probability and converting from an integral to the summation form, we obtain

$$I_\alpha = K \sum_{i=1}^{N} \cos^2 (\theta_i - \alpha)\ P_i \tag{4.16}$$

where P_i is the probability of fibers oriented at angle θ_i interval.

If a web is divided into n direction intervals and current is measured through each interval, we can write the measured current as the probability of fibers in each direction in matrix form

$$AX = B \tag{4.17}$$

where A is the nxn contribution matrix with the entries

$$A_{ij} = \cos^2 \left(\frac{\pi}{n}\ (i-j)\right) \tag{4.18}$$

and B and X are n-tuple vectors. The B vector contains the measured current divided by K in each direction interval. The desired probability values of fibers oriented in each of the n directions are expressed in the X vector. Thus, we must solve this equation for X and the problem becomes one of finding solutions of a set of n simultaneous equations.

4.1.1 The General Anisotropic Case

For the general anisotropic case and any web period (π) divided into 12 direction intervals, Equation (4.17) yields a set of 12 simultaneous equations which may be solved in two steps.

We can normalize the measured currents by any constant since the sum of all probability values is unity. When a period (π) in the web is divided into twelve intervals, the measurement interval is 15 degrees and the matrix A in Equation (4.18) becomes a 12x12 symmetric 3-rank matrix with nine degrees of freedom. Equation (4.17) may or may not have solutions but if it does, an infinite number of solutions exist. If there is no solution, $A^TAX = A^TB$ will have a solution by the convexity argument, but once again an infinite number of solutions exist since A is singular.

Alternatively, since A is a 3-rank matrix, an approximate solution may be obtained by dividing the A matrix into four square matrices, each containing a 60 degree direction interval as shown below:

$$A = \begin{bmatrix} \cos^2 0° & \cos^2 60° & \cos^2 120° \\ \cos^2 120° & \cos^2 0° & \cos^2 60° \\ \cos^2 60° & \cos^2 120° & \cos^2 0° \end{bmatrix} \tag{4.19}$$

The local B values of Equation (4.17) for each group are B1, B2 and B3. Global B values for the first group are B1, B5 and B9, for the second group they are B2, B6 and B10 and so on.

The second step consists of using the approximate values as constraints and employing a nonnegative least square program [24] to find more accurate solutions by performing the operation shown in Equation (4.20).

$$\textit{Minimize} \quad \| EX-f \| \quad \textit{subject to } X \geq 0 \qquad (4.20)$$

where E is the contribution matrix A, X is the fiber orientation distribution, the value we want to find, and f is the current distribution, which has a unique solution by the compactness argument.

4.1.2 The Orthotropic Case

The fiber orientation distribution is orthotropic for many nonwoven materials. For the orthotropic case, Equation (4.17) can be simplified somewhat. The B vector is reduced to 7x1, the X vector is reduced to 7x1, and the global contribution matrix can be superimposed from local contribution factors as shown in Figure 4.1 and it is hence reduced to 7x7 with four degrees of freedom as shown below

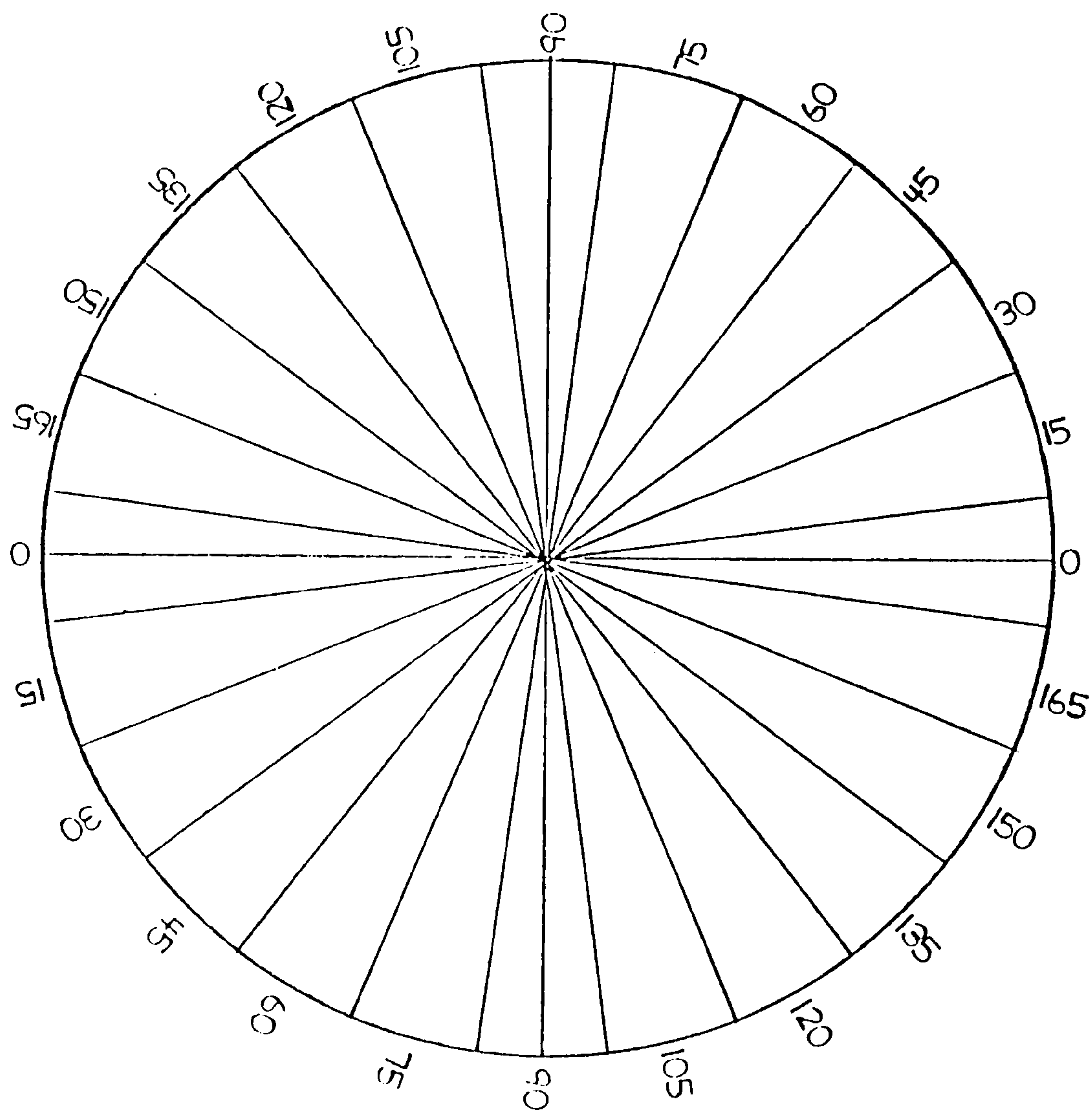

Fig. 4.1 Chart demonstrating the superposition of global contribution matrix from local contribution factors.

$$A = \begin{bmatrix} 1 & 1.866 & 1.5 & 1 & 0.5 & 0.134 & 0 \\ 0.933 & 1.75 & 1.433 & 1 & 0.567 & 0.25 & 0.067 \\ 0.75 & 1.433 & 1.25 & 1 & 0.75 & 0.567 & 0.25 \\ 0.5 & 1 & 1 & 1 & 1 & 1 & 0.5 \\ 0.25 & 0.567 & 0.75 & 1 & 1.25 & 1.433 & 0.75 \\ 0.067 & 0.25 & 0.567 & 1 & 1.433 & 1.75 & 0.933 \\ 0 & 0.134 & 0.5 & 1 & 1.5 & 1.866 & 1 \end{bmatrix} \qquad (4.21)$$

As in the general anisotropic case, the solution to these 7 simultaneous equations may be determined by first finding approximate solutions and then employing a nonnegative least square iteration to obtain more accurate solutions.

4.1.3 The Isotropic Case

To complete this discussion, the isotropic case must be considered. For isotropic materials, measured currents should be equal in every direction interval and the distribution function, $f(\theta)$, should equal some constant. Rewriting the probability density theorem in Equation (4.11) for isotropic materials, we can show the following:

$$\int_{\pi} f(\theta)\, d\theta = 1$$

$$f(\theta) \int_{\pi} d\theta = 1 \qquad (4.22)$$

$$f(\theta) = \frac{1}{\pi}$$

Thus, the fiber orientation distribution function for isotropic materials is characterized by a constant equal to $1/\pi$. In addition, the fiber orientation distribution function may be described as shown below by the second moment $\langle \cos^2\theta \rangle$, which is 1/2 for isotropic webs.

$$\int_{\pi} \cos^2\theta \, f(\theta) d\theta = \overline{\cos^2\theta} = I/K$$

$$\overline{\cos^2\theta} = \frac{1}{\pi} \int_{o}^{\pi} \cos^2\theta \; d\theta \tag{4.23}$$

$$\overline{\cos^2\theta} = \frac{1}{2}$$

4.2 Instrumentation

Hearle [25] showed that moisture and temperature significantly affect the electrical resistance of textile materials. Figures 4.2 and 4.3 show the effect of temperature and moisture on resistance, respectively. Hersh and Montgomery [26] designed a sample chamber and an electrical circuit to measure the resistance of textile materials. However, the measurements were restricted to natural fibers because of inadequate sample chamber design and inaccuracy of contemporary electrical instruments.

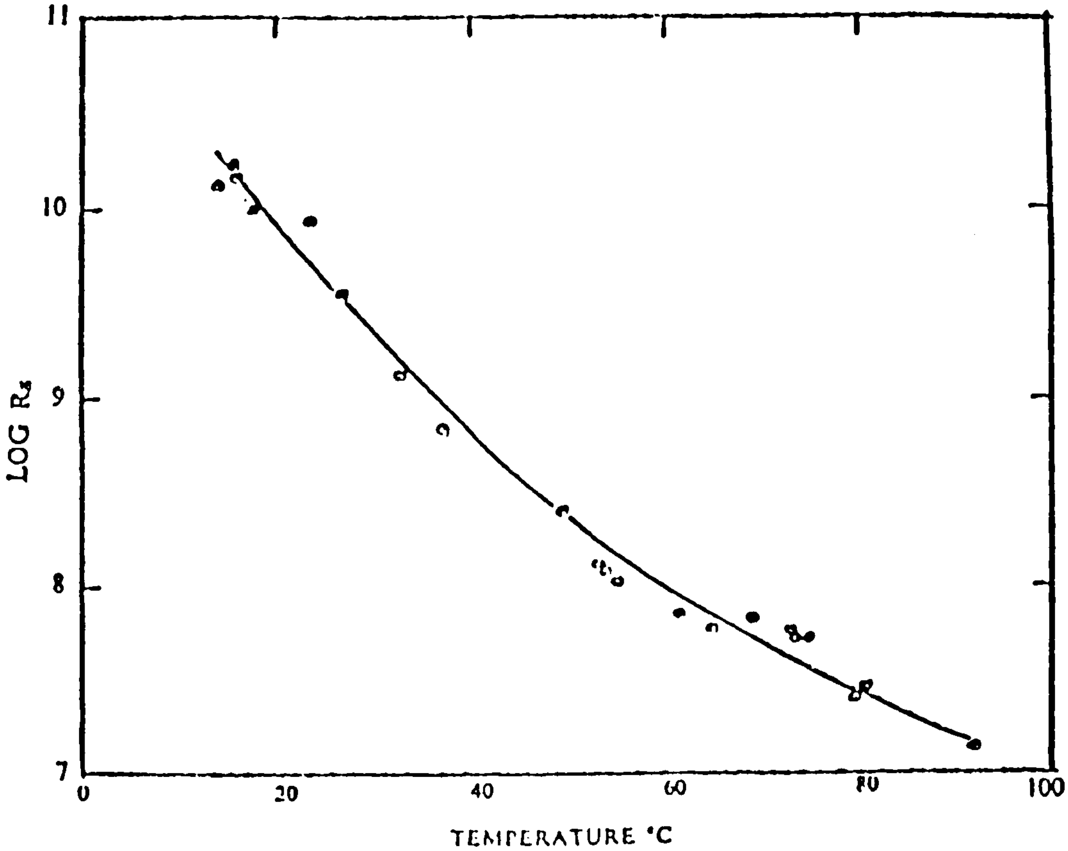

Fig. 4.2 Variation of nylon resistance with temperature at 6% moisture content [25].

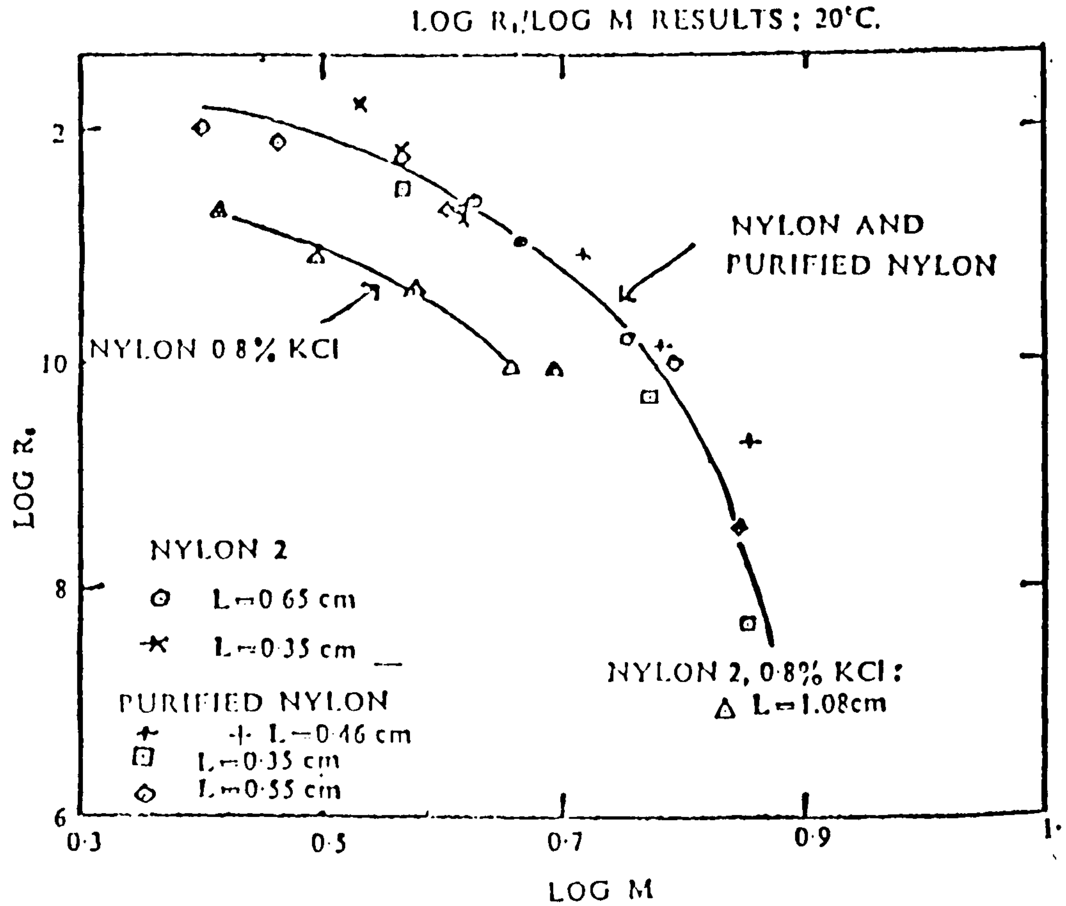

Fig. 4.3 Variation of resistance with moisture content at 20°C [25].

Several techniques have been developed to measure the resistance of high-resistance materials. These include the Wheatstone bridge, the voltage divider, the RC circuit and the electrometer. Because of recent progress in electronics, the electrometer is the most accurate way to measure the resistance of high-resistance materials and it was used in this Dissertation.

Figure 4.4 shows the sketch of our first generation instrument. Sample length was adjustable in this design. The sample holder was supported by high-resistance plastic rods which sat on a high-resistance board at a distance far away from the sample. The whole sample holder was placed in a plexi-glass box and a pair of plastic gloves was used to change samples. Figure 4.5 shows the variation of current with the action of the room humidifier and dehumidifier. This proves that the plexi-glass chamber was unable to control humidity to the degree required for good electrical current measurement.

The second generation instrument was specifically designed to control the relative humidity in the sample chamber. Twelve sample holders were placed in a chamber as shown in Figure 4.6. The chamber was immersed in a jar filled with water. The water temperature in the jar was maintained by a thermostat controlled heater. A saturated salt solution was put in the chamber to maintain constant

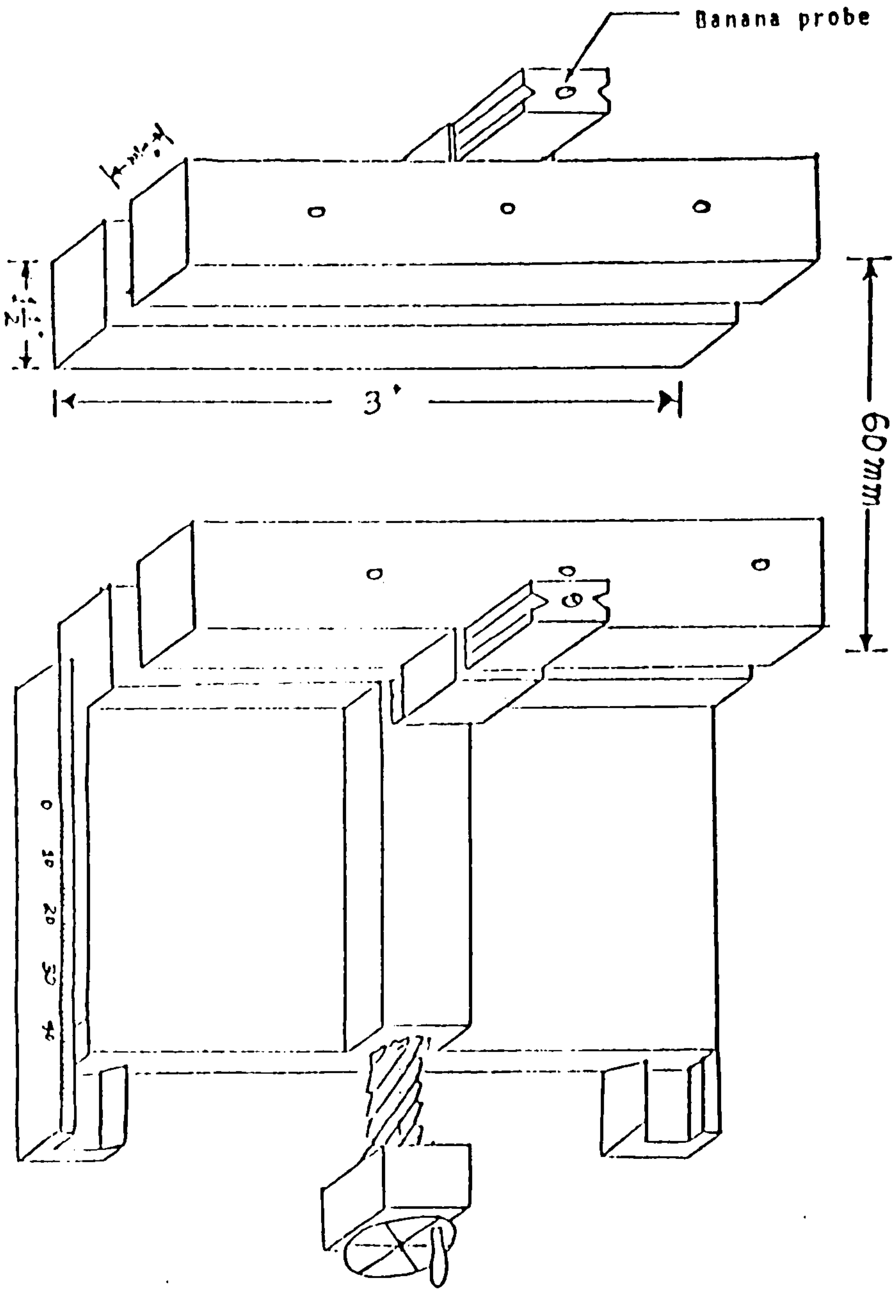

Fig.4.4 First generation instrument allowing variable sample length.

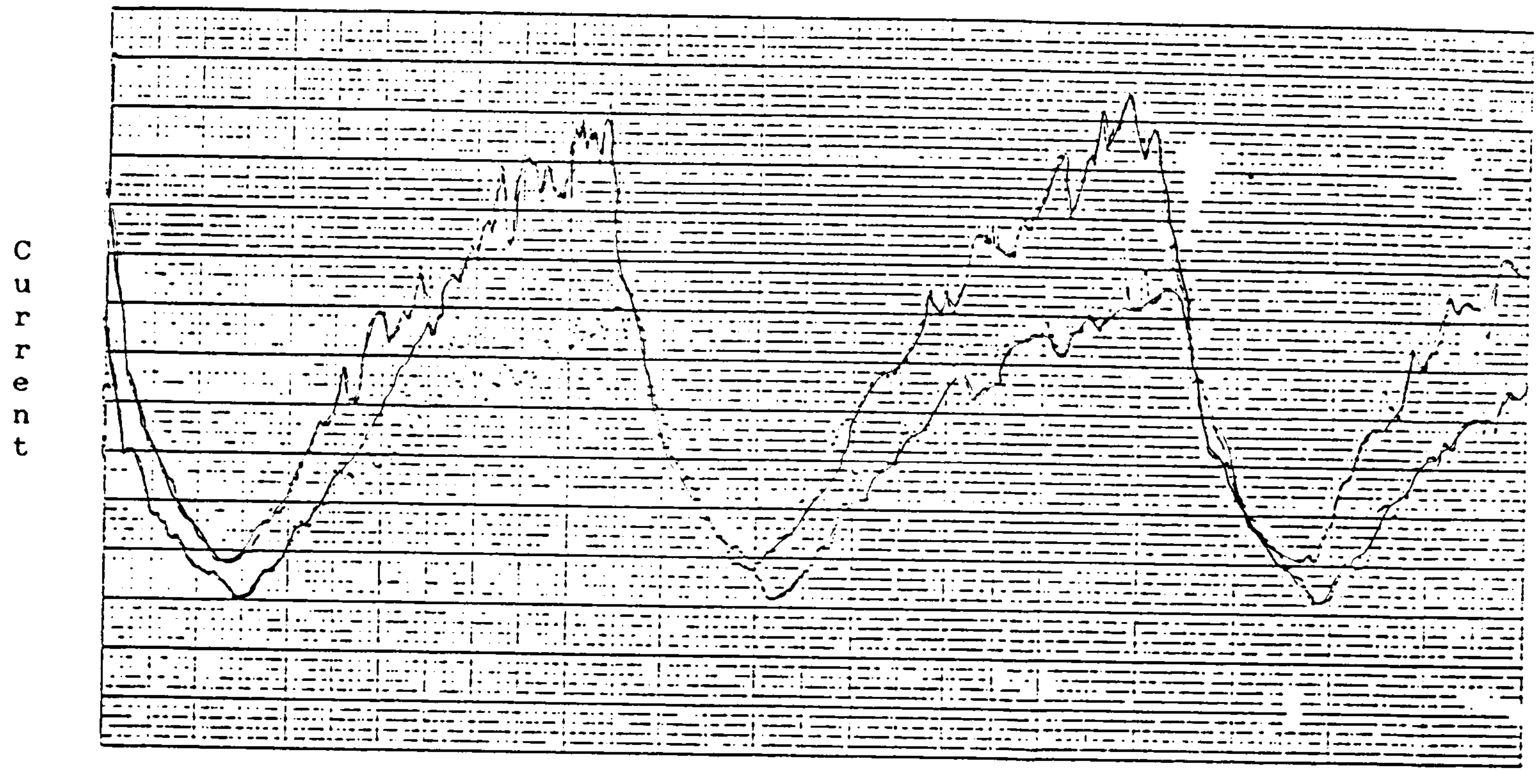

Fig. 4.5 Dependence of measured current on action of the humidifier and dehumidifier.

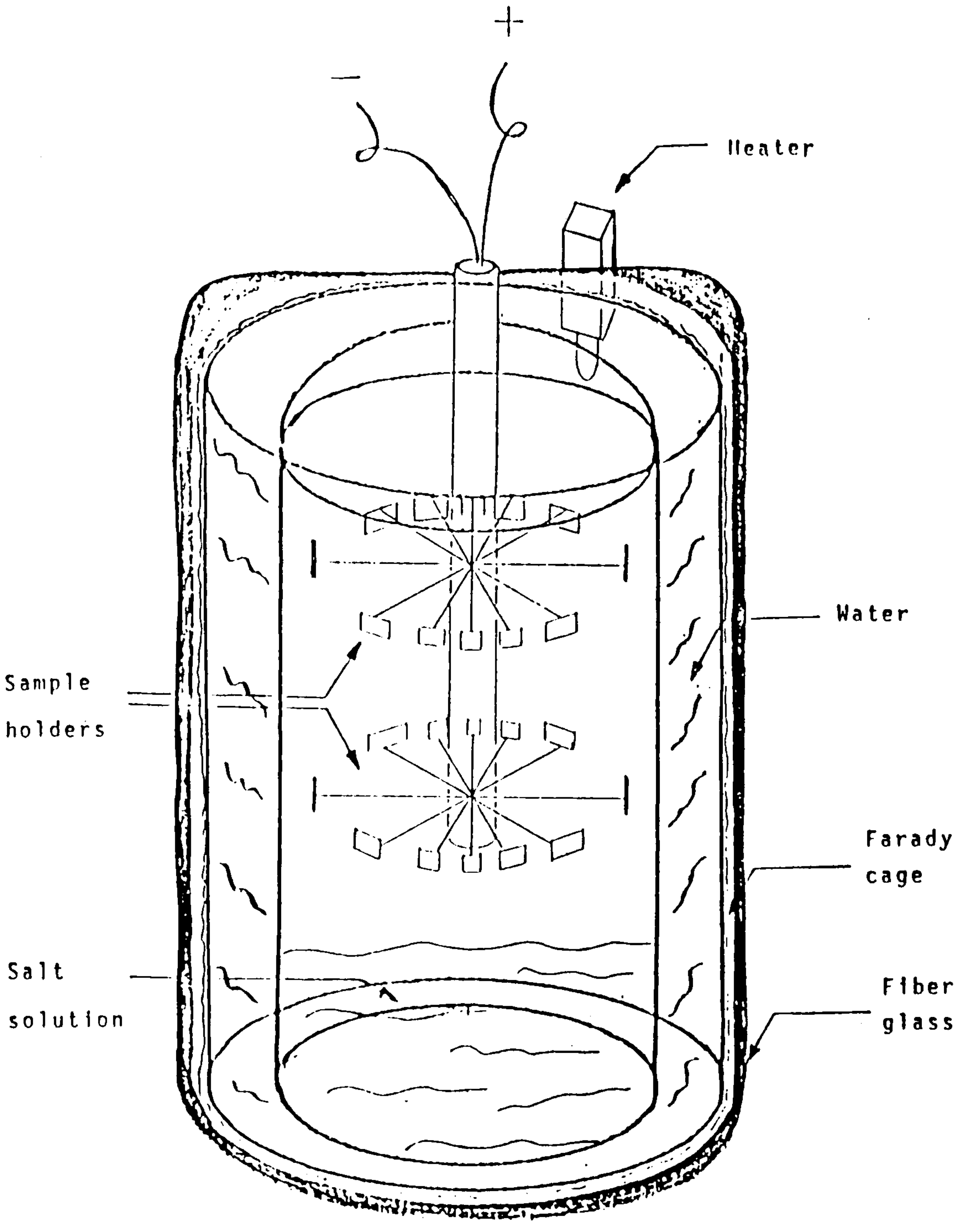

Fig. 4.6 Second generation instrument adding control of relative humidity in the chamber.

relative humidity at a constant temperature [27]. The problem with this instrument design was that the voltage-supply wire interfered with the wire which was used to draw current through the sample. Another design problem was that water in the jar did not cover the whole sample chamber. Water vapor thus condensed on the chamber top and occasionally dropped into sample.

Failure is the mother of success. The third generation instrument was built to strictly control relative humidity and to shield the applied field from interference. The sample chamber and sample holder were deliberately designed to match the electrometer. The electrical circuit is shown in Figure 4.7 and the whole instrument system is shown in Figure 4.8. In this instrument system, a high voltage power supply and a Keithley Model 617 programmable Electrometer which was specifically designed for current measurements from high resistance materials were used. The sample chamber contained twelve sample holders so twelve sample direction intervals could be measured without disturbing the environmental conditions within the chamber.

The temperature in the chamber was controlled by immersing the whole chamber in a large jar filled with water whose temperature was controlled with an immersion heater. This allowed temperature control in the sample chamber to within $\pm$ 0.1^{0}C. A saturated salt solution was placed on the

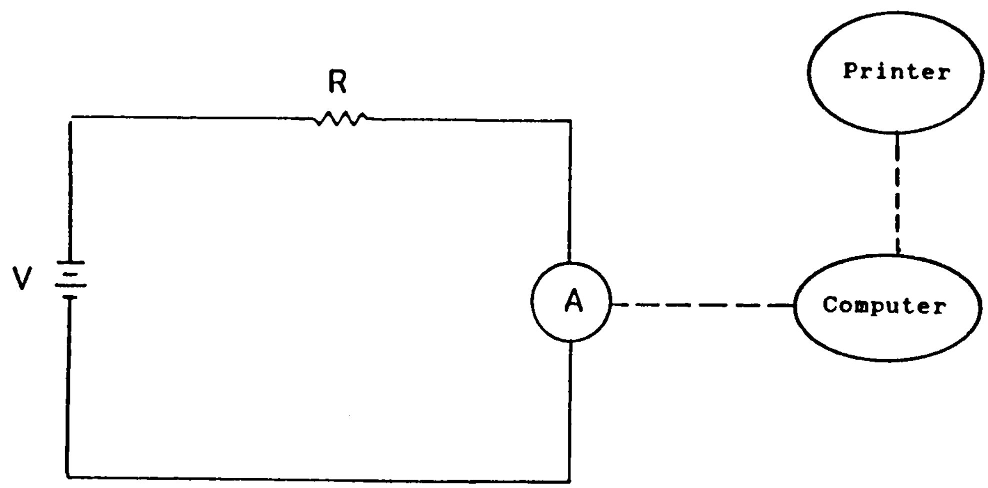

V: High voltage power supply (Keithley Model 247)

R: Sample and sample holder

A: Multi-use electrometer (Keithley Model 617)

Fig. 4.7 Electrometer circuit for determining the fiber orientation distribution.

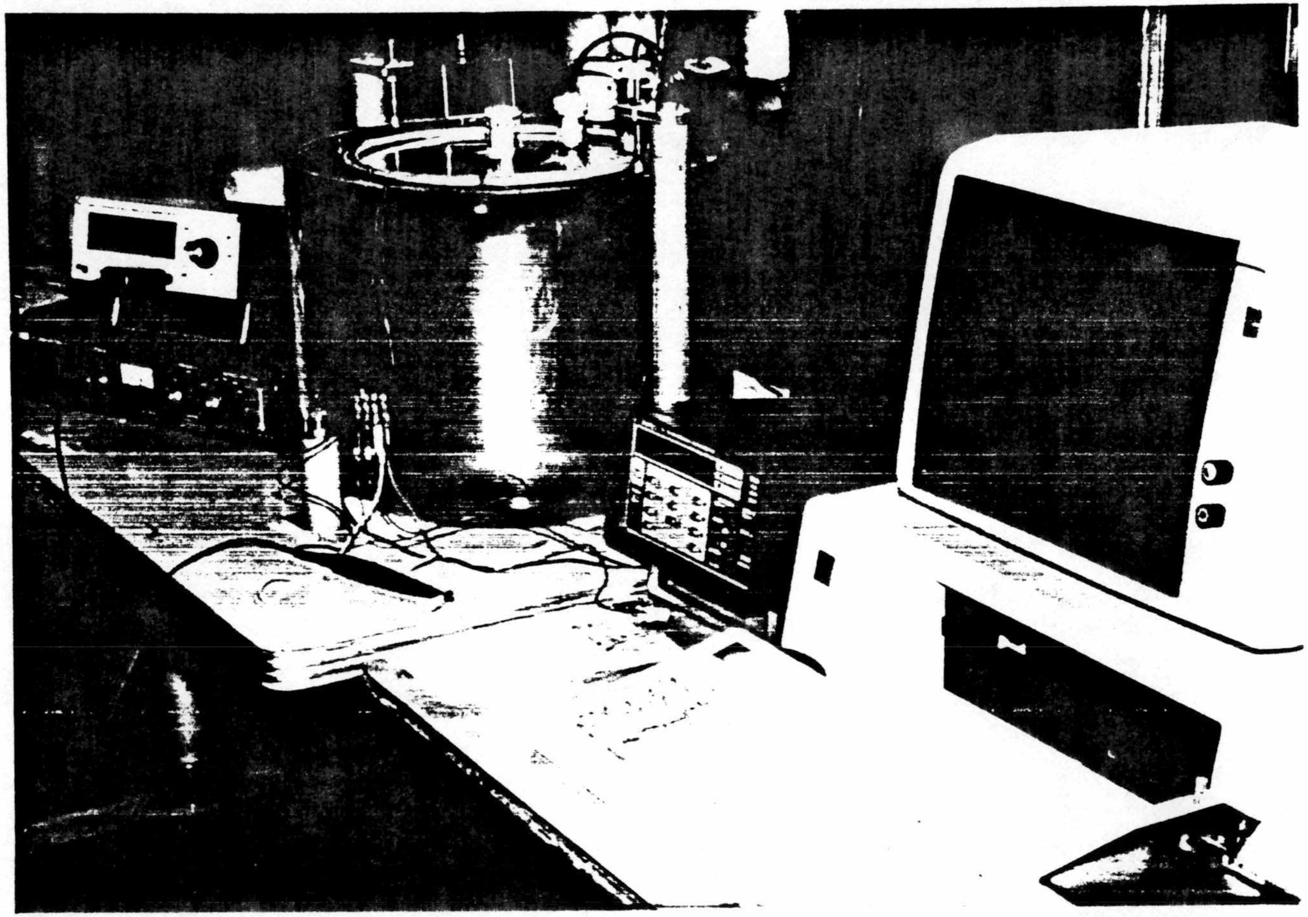

Fig. 4.8 Illustration of third generation instrument system that measures the currents of high-resistance materials.

bottom of the chamber to maintain a constant relative humidity [27] as shown in Figure 4.9. An Omega transmitter was put inside the sample chamber to measure the temperature and relative humidity. After equilibrium was reached, the relative humidity was controlled to within ± 0.5% R.H.

Samples were held by two clamps unconnected by any support frame as shown in Figure 4.10 so current could not travel around the samples by passing through the frame. The whole chamber was covered by metal which functioned as a Faraday cage to shield the apparatus from electrical field interference. All connections were through coaxial cable for additional shielding. The wave guide of the electromagnetic waves produced by the current in the coaxial cable is transverse electric and magnetic field. The electric field originates from the center wire, propagates radially and finally sinks to the outer wires.

Since the sample holder configuration in the circuit functioned as both a resistor and a capacitor, the current was not immediately stable upon closing any switch. The time needed to attain current equilibration depended on the capacitance and other factors, but usually was found to be less than two minutes. Finally, the electrometer was connected to a computer for multiple data acquisition so that, once equilibration was achieved, current values could be collected to provide an average current measurements.

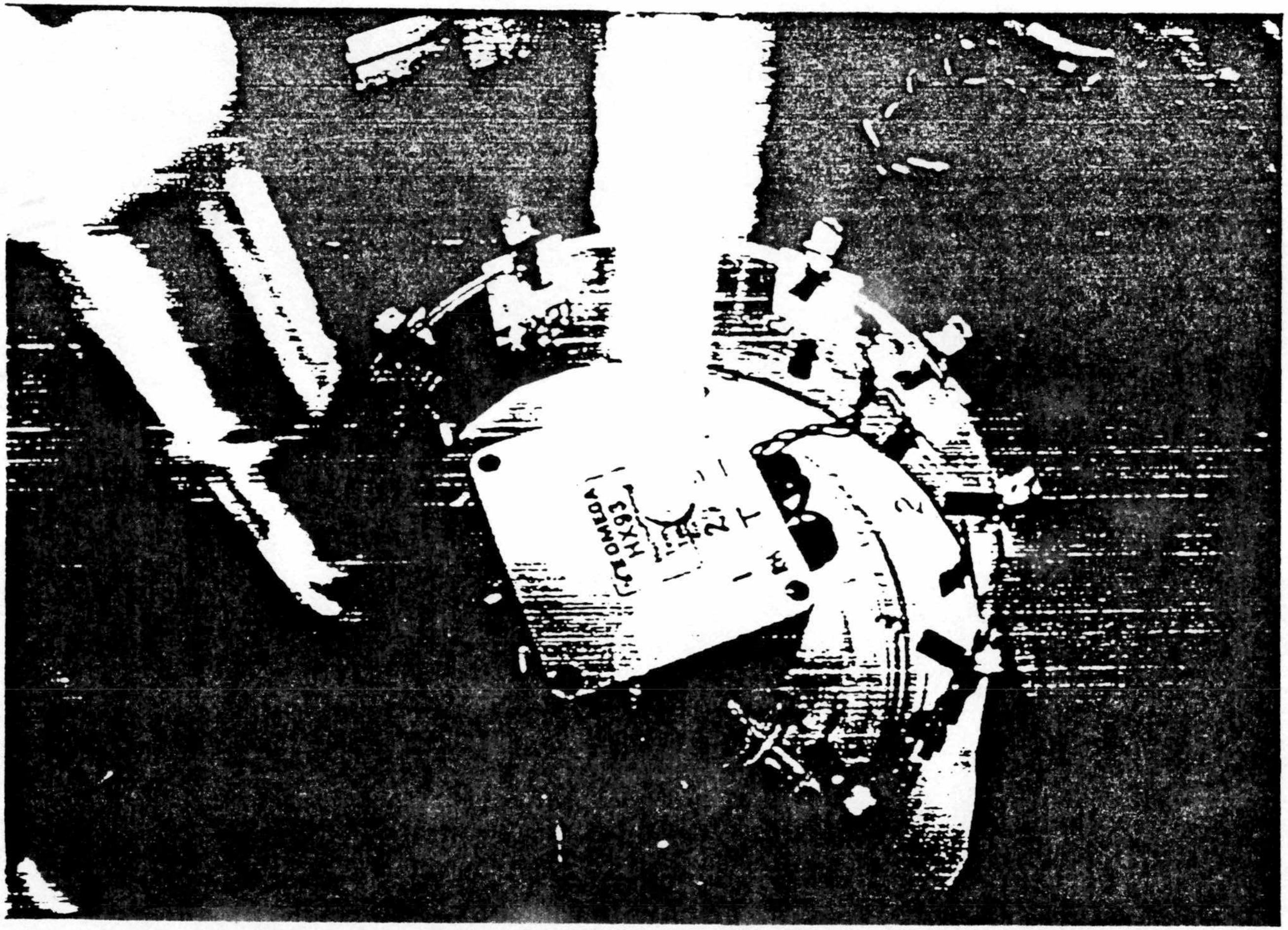

Fig. 4.9 Inside of the chamber shows the saturated salt solution on the bottom and an Omega transmitter for measuring temperature and relative humidity.

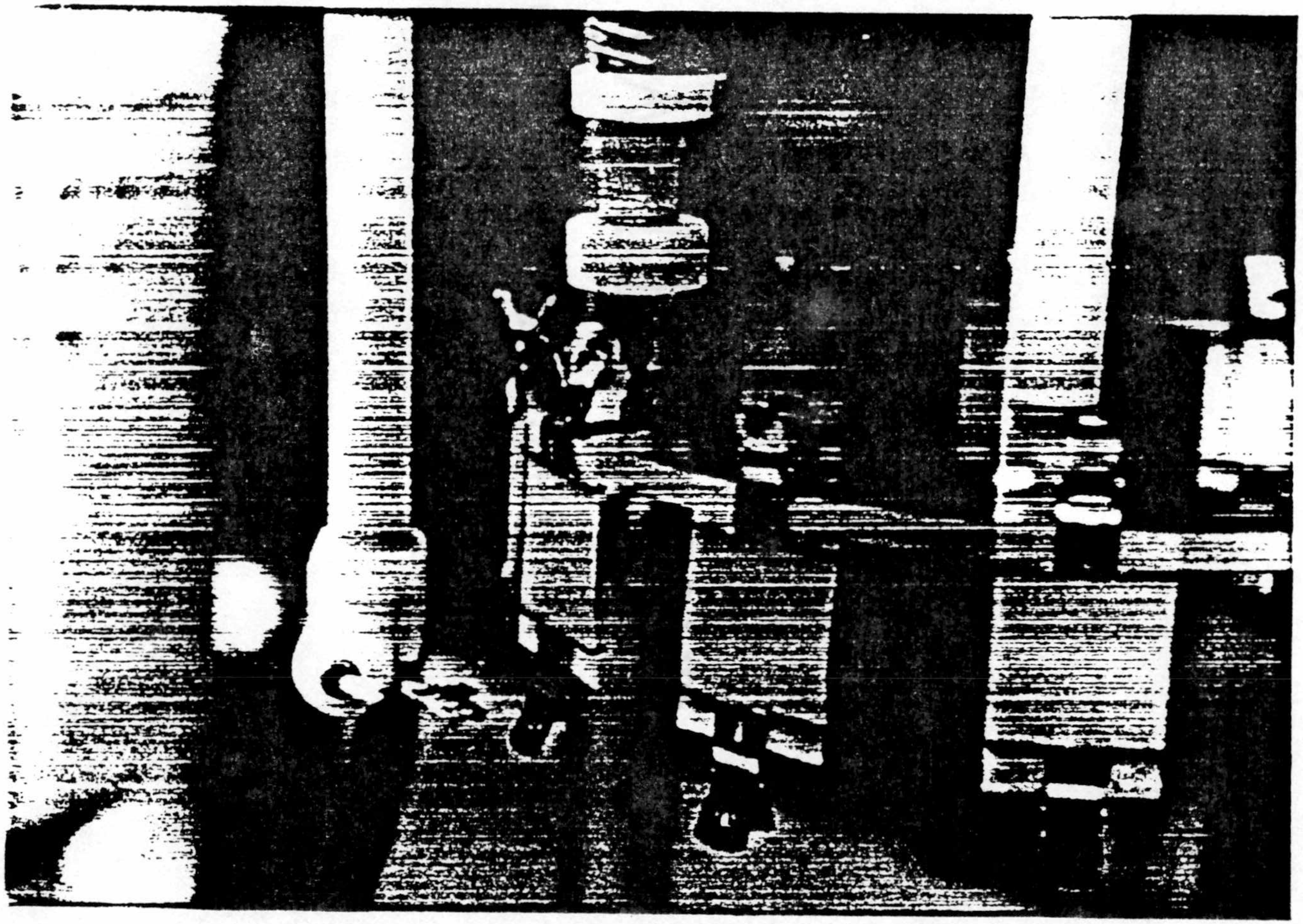

Fig. 4.10 A close look at the sample holder. High voltage is supplied by the top brush and current is drawn by the bottom brush.

CHAPTER 5

EXPERIMENTAL

Samples were prepared using the melt blown pilot line at the University of Tennessee. The basic configuration of this line is shown in Figure 5.1. Webs having different fiber-orientations can be produced by changing processing conditions such as the distance between die and collector (DCD), air valve opening, collector speed and collector height.

By choosing various combinations of processing conditions, three nylon webs were produced which exhibited low, medium, and high fiber orientations. Processing conditions used to make these webs are described in Table 5.1. and Figures 5.2-5.4 show optical photomicrographs of the low-, medium- and highly-oriented webs, respectively.

A protractor template as shown in Figure 5.5 was used to cut twelve specimens in 15-degree direction intervals from each web. All twelve specimens from a single web were placed in the sample chamber simultaneously. After temperature and humidity equilibration was attained (approx. 48 hours), voltage was successively applied to each specimen while current conducted through each specimen was recorded 30 times in rapid succession. The current conducted through

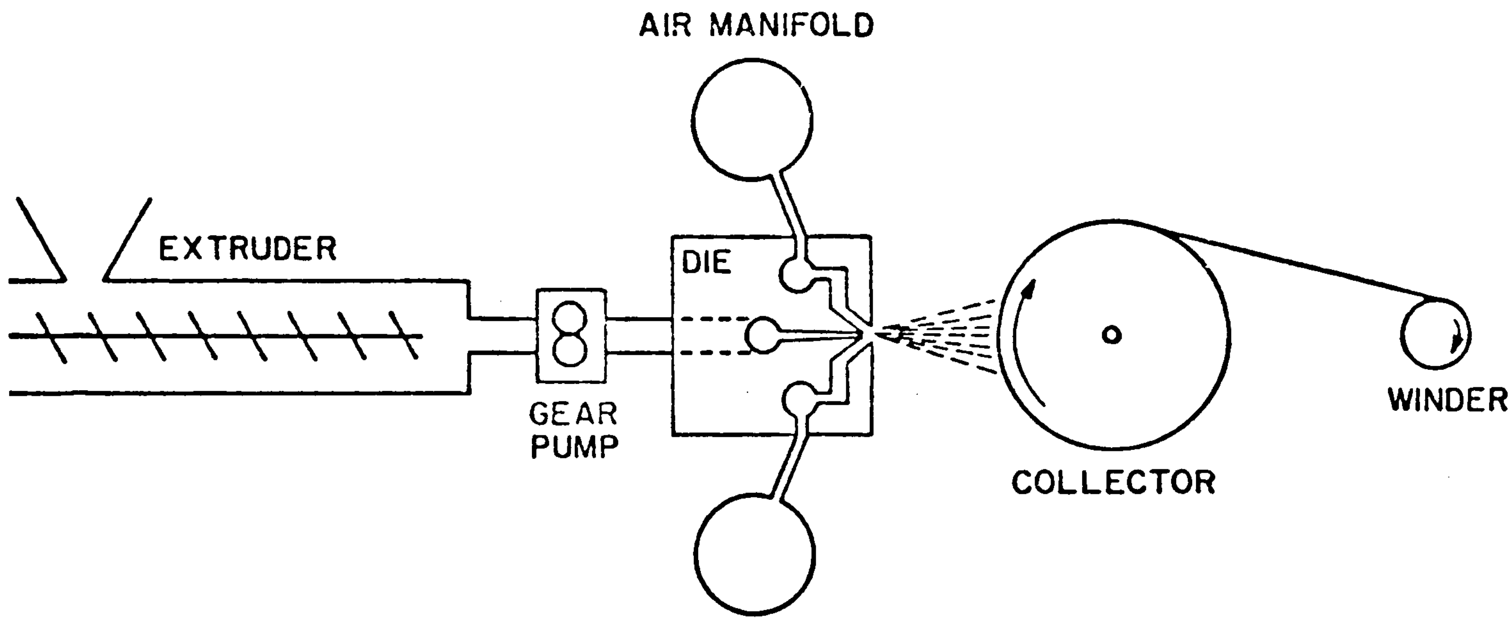

Fig. 5.1 Melt blown pilot line at the University of Tennessee.

Table 5.1 Processing conditions to make three different fiber-oriented webs.

Polymer: Nylon 6 from BASF

Throughput: 0.4 g/hole/min.

Fiber Orientation	Low	Medium	High
Web Basis Weight (oz/yd^2)	0.711	0.934	0.329
Air Valve Opening (%)	90	55	55
Collector Speed (ft/min)	50	30	70
DCD (inch)	8	8	8
Collector Position	middle	middle	middle

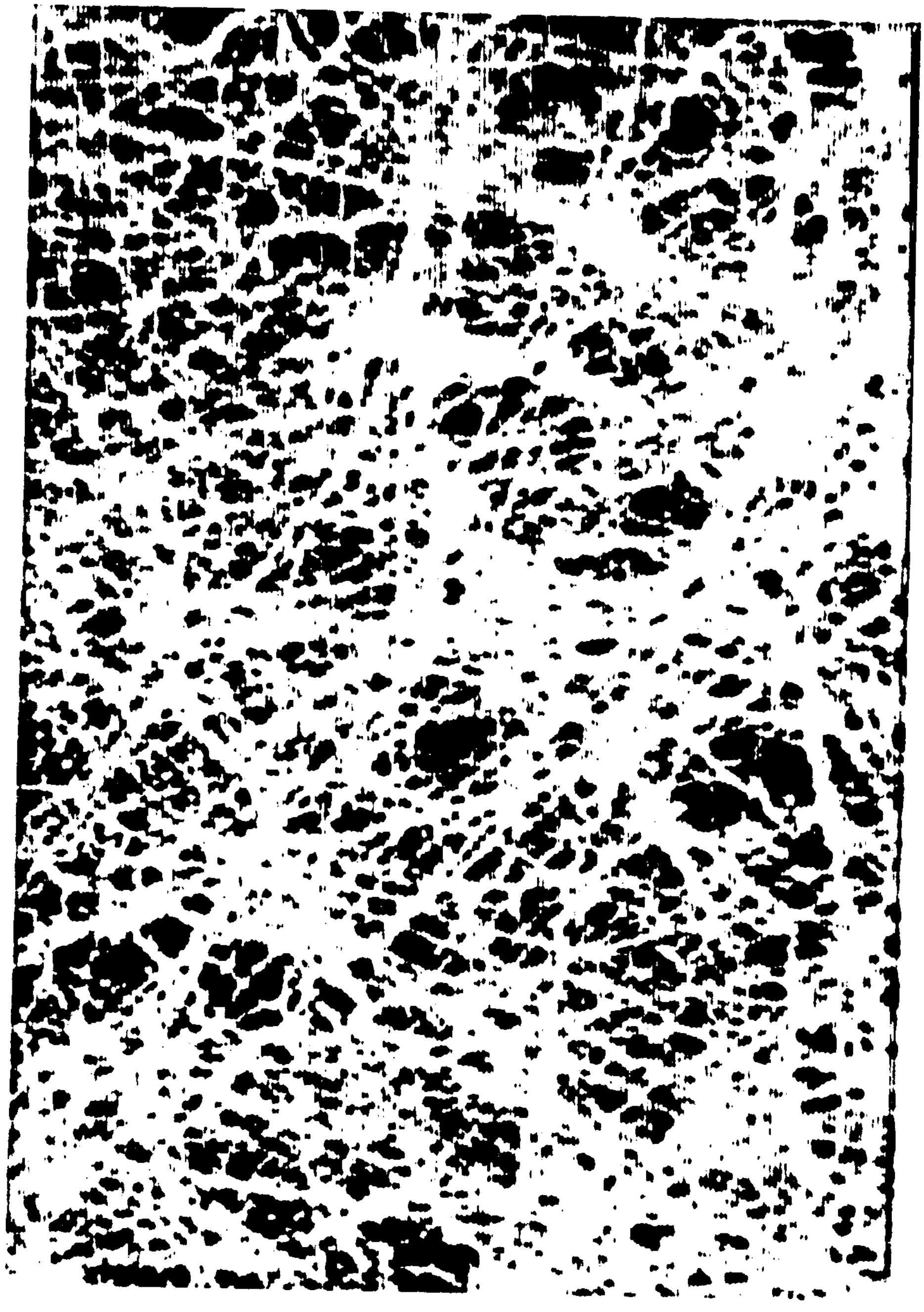

Fig. 5.2 Photomicrograph of low-oriented web.

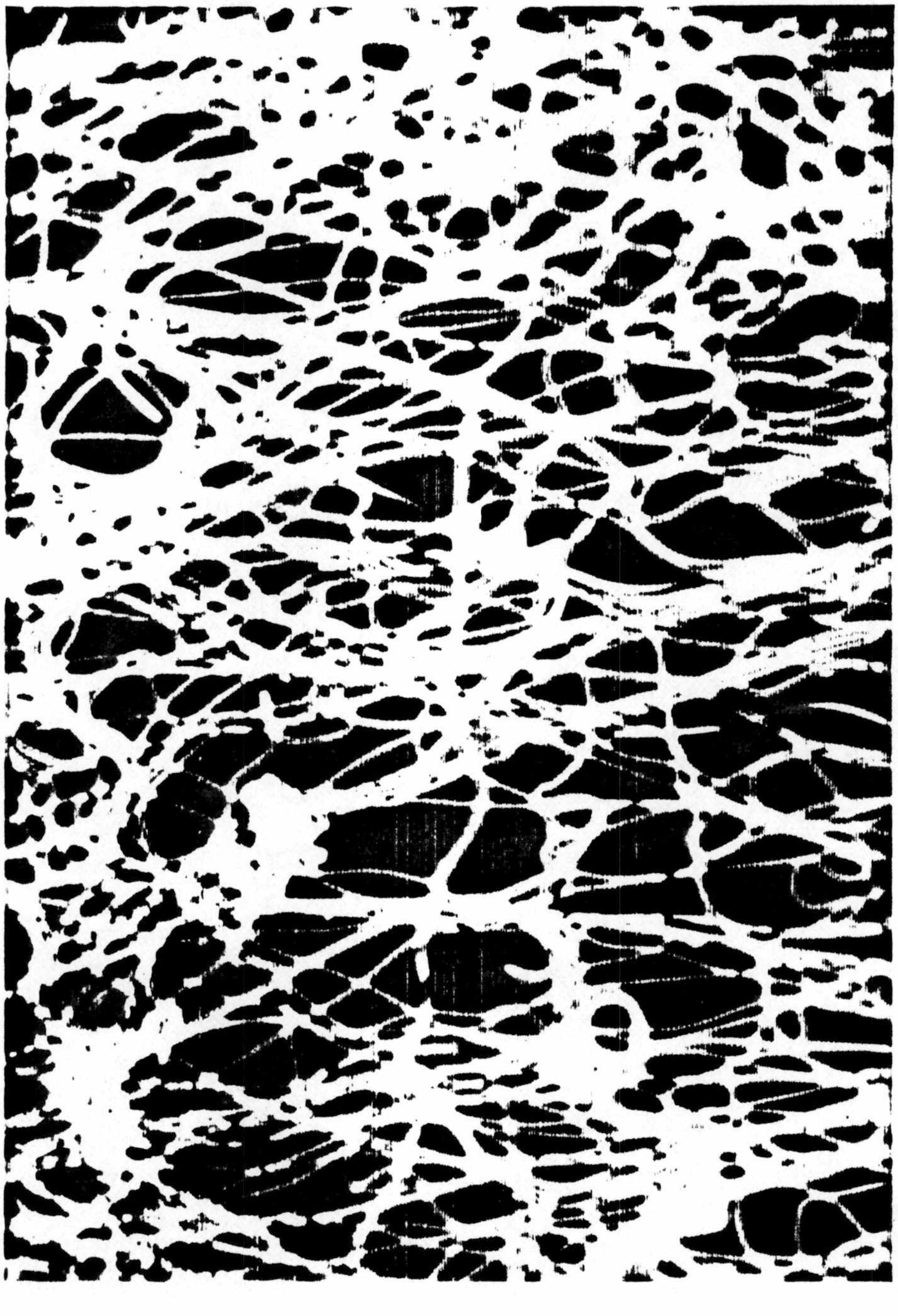

Fig. 5.3 Photomicrograph of medium-oriented web.

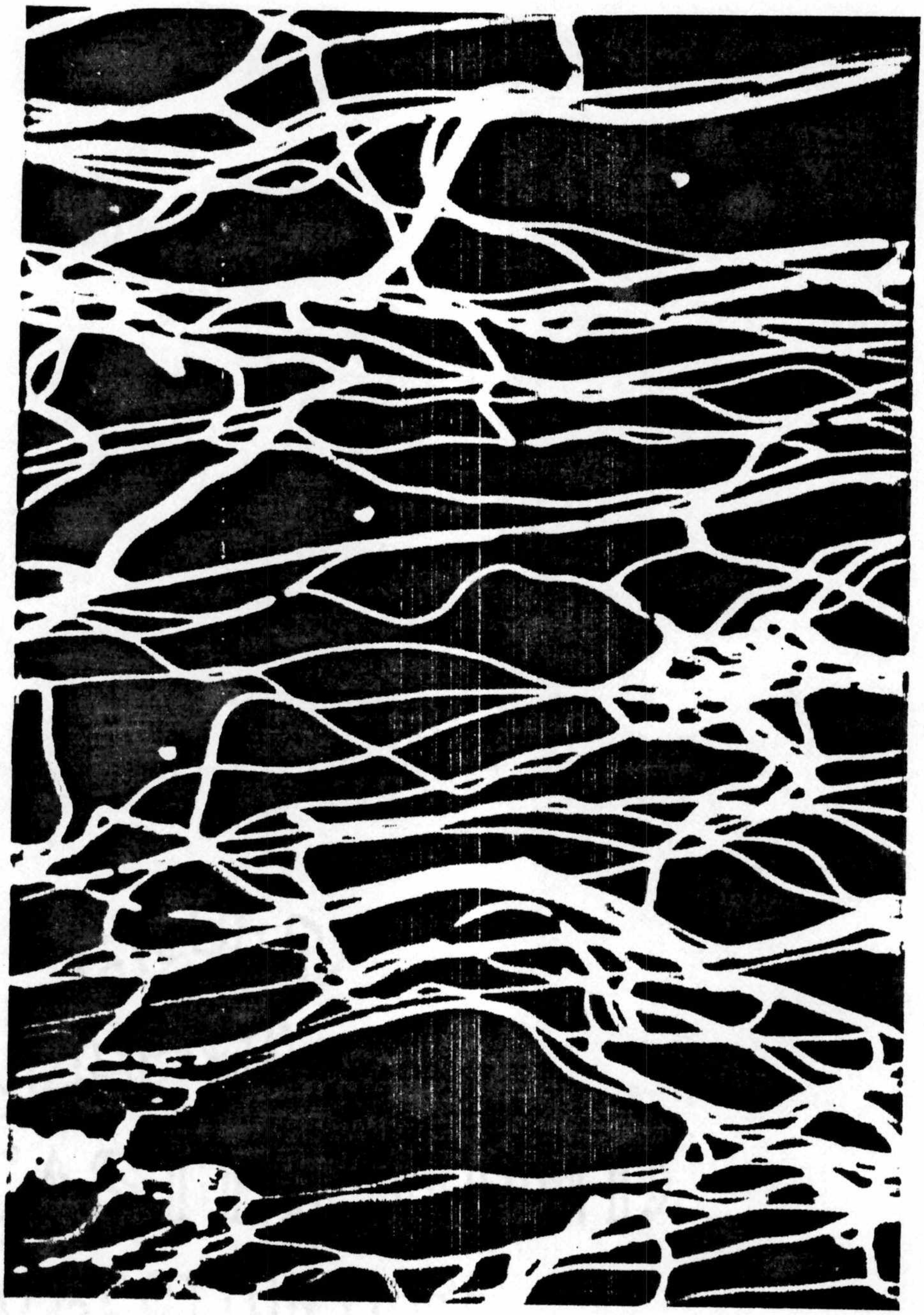

Fig. 5.4 Photomicrograph of highly-oriented web.

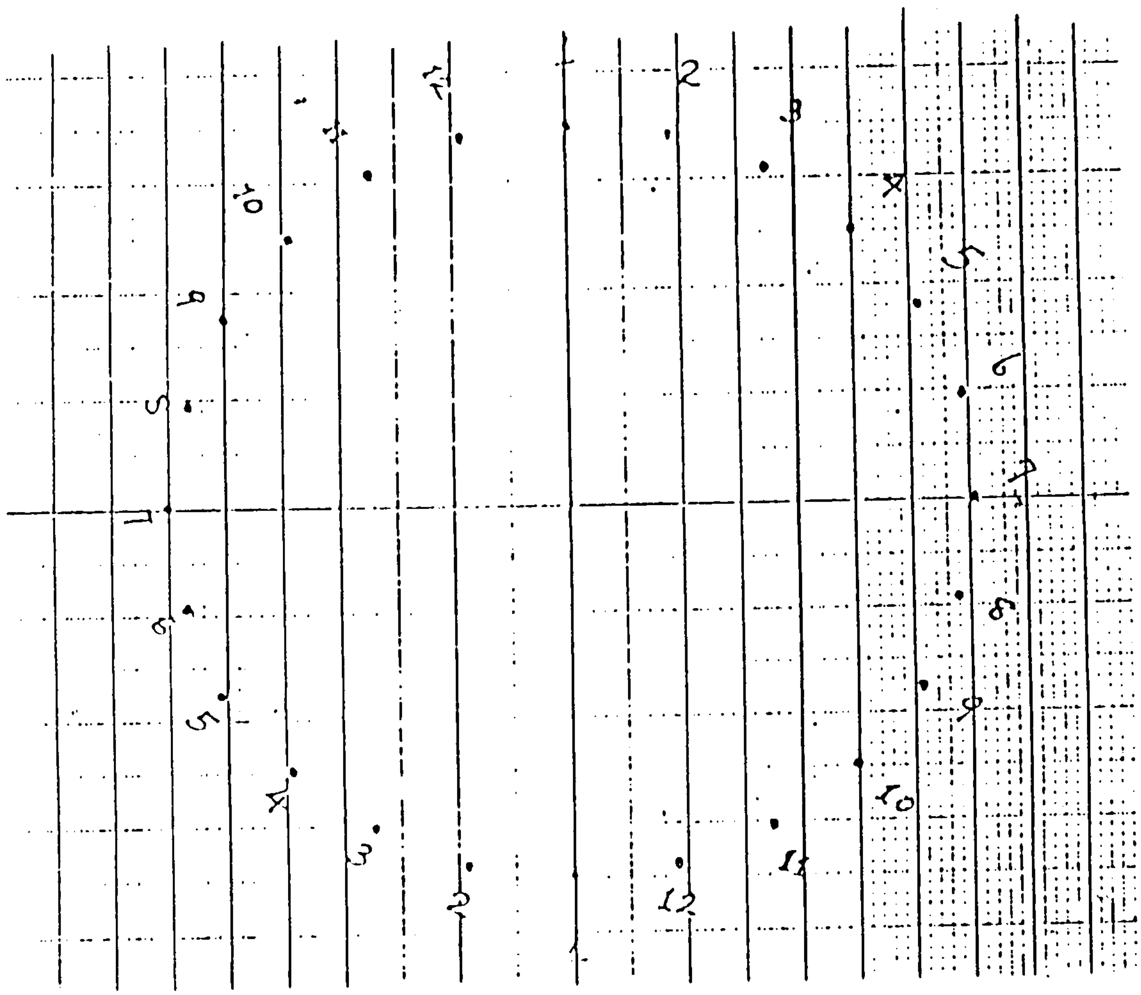

Fig. 5.5 A protractor template was used to cut twelve specimen in 15-degree direction intervals.

each specimen was recorded an additional 30 times and, then, a final 30 times. The three groups of 30 data points were averaged and the current distribution among the 12 direction intervals of a web was calculated using Program1 in the Appendix.

The current distribution thus obtained was used to compute the fiber orientation distribution using Program2 and Program3 in the Appendix according to the theory developed in Section 4.1 Finally, fiber-web theory was applied to the fiber orientation distribution to obtain theoretical compliance constants using Program4 in the Appendix.

Specimens for mechanical testing measuring 7"X1" were cut using a die. Only axial compliance constants were determined by mechanical testing so constraints on specimens would not reduce testing accuracy by Saint-Venant's principle [16,28]. Although creep was ignored during tensile testing, a relatively slow cross-head speed of 2.54 cm/min was used to prevent web catastrophic failure. Program4 in the Appendix was used to calculate and normalize compliance constants from tensile testing data. These normalized web compliance constants were compared with theoretical compliance constants computed from electrical measurements using fiber web theory to test the validity of the electrical measurements and theory developed.

The highly-oriented web was too thin to measure compliance constants from tensile testing reliably. Instead, the actual fiber orientation distribution of this web was determined by counting the number of fibers aligned in various directions when the web was magnified with a projecting microscope. Since this web was characterized by a large variation in fiber diameter, an equivalent number of fibers was estimated from the fiber diameter, D, and number counted, n, by

$$Eq.\ number = n\left(\frac{\pi D^2}{4A_r}\right) \tag{5.1}$$

where A_r is a unit reference area. It seemed prudent to take fiber diameter into account in this way since stress is force divided by cross-sectional area and the fiber orientation distribution determined by electrical measurements takes cross-sectional area into account as mentioned in Chapter 3.

CHAPTER 6

RESULTS AND DISCUSSION

Different specimen lengths (0.5", 1" and 2") and various applied voltages (1, 2 and 3 kV), were evaluated to test if Ohm's law was obeyed. Experiments showed that measured current was proportional to applied voltage and was approximately inversely proportional to specimen length. The current was not exactly inversely proportional to specimen length as predicted by Equation (4.1), apparently because webs were not uniform and the average fiber orientation varied when the specimen length changed. However, Ohm's law was, in principle, obeyed for the applied voltages and specimen lengths tested. A specimen length of 0.5" and applied voltage of 2 kV were selected for all subsequent measurements.

A sample chamber temperature around 30^0C and relative humidity around 60% RH were selected. Temperature and humidity changed slightly when the sample chamber was opened and current measurements changed. Figure 6.1 shows how measured currents from one web sample vary for three different temperature and humidity conditions. However, the current distribution remained constant for the same samples at different temperature and humidity conditions once

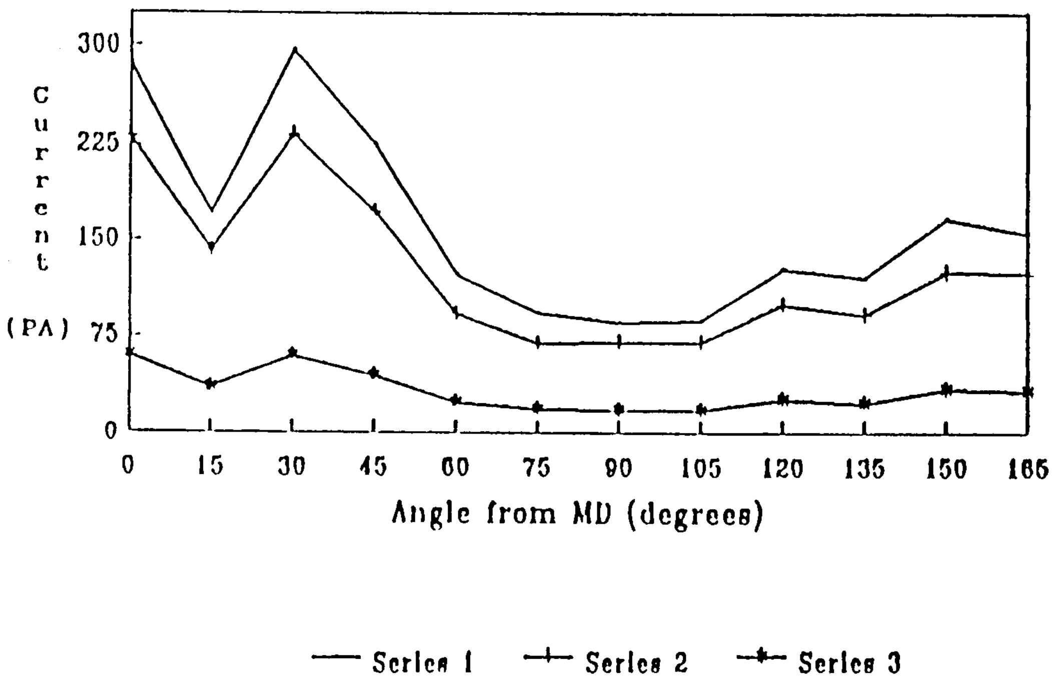

series 1 - 33.4 C, 60.6 %RH, 40 hours
series 2 - 33.3 C, 59.5 %RH, 95 hours
series 3 - 23.7 C, 58.0 %RH, 24 hours

Fig. 6.1 Currents measured at various temperature and relative humidity show the effect of measurement conditions.

temperature and humidity equilibrium was achieved. When the currents in Figure 6.1 are plotted as current distributions as shown in Figure 6.2, it can be seen that current distribution is independent of temperature and humidity.

Table 6.1 shows fiber orientation distributions of the low, medium and highly oriented webs computed from electrical measurements using the theory described in Chapter 4. When converting measured electrical currents to the fiber orientation distribution, orthotropic properties were assumed for low- and medium-oriented webs. This seemed justified when considering the values in Table 6.1 since current was symmetric about the machine and cross directions.

A simple measure of fiber orientation can be obtained from the relative distribution of fibers between machine and cross directions. This ratio is 10.6/6.0 = 1.8, 15.3/1.11 = 13.8, and approximately 18.4/0.2 = 92 for the low, medium and highly-oriented webs, respectively. The ratio can be seen to increase with increasing anisotropy of the webs. When comparing these ratios and the data in Table 6.1 to photomicrographs of the webs (Figures 5.2-5.4), good qualitative agreement is evident.

Table 6.2 shows the actual fiber orientation distribution of the highly-oriented web obtained by counting fibers and converting counts to equivalent fibers by

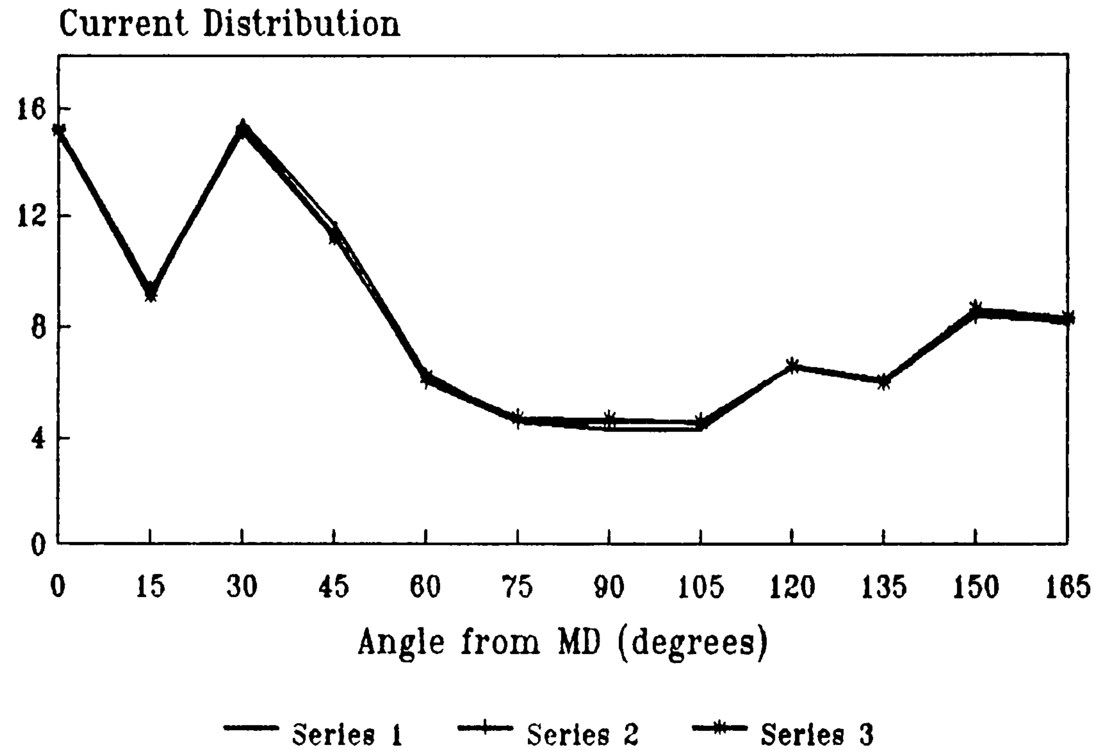

series 1 - 33.4 C, 60.6 %RH, 40 hours
series 2 - 33.3 C, 59.5 %RH, 95 hours
series 3 - 23.7 C, 58.0 %RH, 24 hours

Fig. 6.2 Current distribution from various measurement conditions.

Table 6.1 Fiber orientation distribution of three webs from electrical measurements.

Angle from M/D (degrees)	Low Oriented	Medium Oriented	Highly Oriented
0	10.6	15.3	19.8
15	9.8	13.1	18.5
30	9.1	10.7	15.1
45	8.3	8.4	10.7
60	7.6	6.0	3.2
75	6.9	3.6	0.3
90	6.0	1.1	0.0
105	6.9	3.6	0.0
120	7.6	6.0	2.9
135	8.3	8.4	4.6
150	9.1	10.7	11.3
165	9.8	13.1	13.8

Table 6.2 Fiber orientation distribution of highly oriented web from fiber counting.

Angle from M/D (degrees)	Highly Oriented
0	18.4
15	17.4
30	14.9
45	11.5
60	1.2
75	0.2
90	0.0
105	0.3
120	1.0
135	8.8
150	11.8
165	14.6

Equation 5.1 when the webs were viewed with a microscope. When comparing this fiber orientation distribution to that obtained from electrical measurements (Table 6.1), good agreement is evident. Some deviation is evident, however, at and near the cross direction. This probably resulted from the small number of fibers in that direction for the highly-oriented web.

Table 6.3 shows normalized axial compliance constants of the three webs computed from fiber-web theory using the fiber orientation distributions in Table 6.1 which were obtained from electrical current measurements. The cross direction, machine direction compliance ratios are 9.7/7.1 = 1.4, 13.4/4.8 = 2.8, and 18.0/2.4 = 7.5 for the low, medium and highly-oriented webs, respectively. Like the fiber orientation ratio, the compliance ratio increases with increasing web anisotropy.

It is instructive to compare the ratios of fiber orientation distribution and compliance constants. Not only are these two ratios not equivalent but they exhibit large differences. This can be explained because the fiber orientation distribution is a statistical measure of fibers in each direction whereas the elastic constant in any web direction results from the contribution of fibers in all web directions as discussed previously in Section 3.2.

Table 6.3 Normalized axial compliance constants of three webs computed from fiber-web theory using fiber orientation distributions obtained from electrical measurements.

Angle from M/D (degrees)	Low Oriented	Medium Oriented	Highly Oriented
0	7.1	4.8	2.4
15	7.3	5.0	2.4
30	7.7	5.8	2.8
45	8.3	7.6	5.0
60	8.9	10.1	9.7
75	9.5	12.5	15.0
90	9.7	13.4	18.0
105	9.5	12.5	17.1
125	8.9	10.1	12.8
135	8.3	7.6	8.3
150	7.7	5.8	4.0
165	7.3	5.0	2.6

Table 6.4 shows normalized axial compliance constants measured from tensile testing. The highly-oriented web, however, was too thin to measure its axial compliance constants by tensile testing, so they were computed from fiber-web theory using the actual fiber orientation distribution determined by fiber counting. The validity of the testing instrument and theory developed can be assessed by comparing compliance constants computed from electrical measurements (Table 6.3) with actual compliance constants computed from tensile testing and fiber counting (Table 6.4). Excellent agreement can be seen.

To facilitate comparisons, the data in Tables 6.3 and 6.4 are plotted in Figures 6.3-6.5. for low- medium- and highly-oriented webs, respectively. Figures 6.3 & 6.4 show the excellent agreement between axial compliance computed from electrical measurements and determined by tensile testing for the low and medium oriented webs. Figure 6.5 shows good agreement between axial compliance computed from electrical measurements and from counting fibers for the highly oriented web. Differences between compliance constants are relatively small, being only a few percent. In the machine direction, deviations are (7.3 - 7.1) / 7.3 = 2.7%, (4.8 - 4.6) / 4.8 = 4.2%, and (2.4 - 2.4) / 2.4 = 0% for the low, medium, and highly-oriented webs, respectively. In the cross direction, deviations are (9.7 - 9.7) / 9.7 =

Table 6.4 Normalized axial compliance constants from tensile testing and from counting fibers under microscope.

Angle from M/D in Degrees	Tensile testing		Counting
	Low Oriented	Medium Oriented	highly Oriented
0	7.3	4.6	2.4
15	7.4	4.9	2.2
30	7.9	5.6	2.7
45	8.4	7.8	5.4
60	8.8	10.2	10.6
75	9.7	12.1	16.3
90	9.7	13.2	19.0
105	9.2	12.5	17.2
120	8.4	10.6	12.0
135	8.6	8.4	6.5
150	7.6	6.0	3.3
165	7.1	4.2	2.4

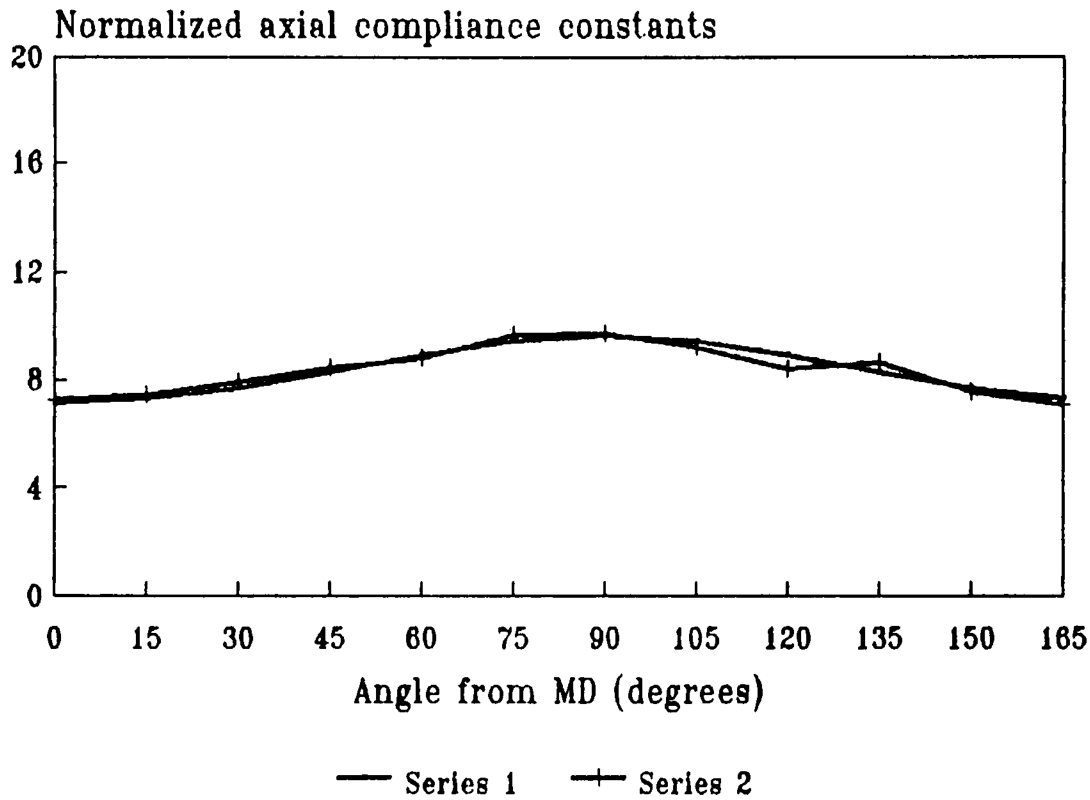

series 1 - from electrical measurements
series 2 - from tensile measurements

Fig. 6.3 Comparison of normalized axial compliance constants of low-oriented web.

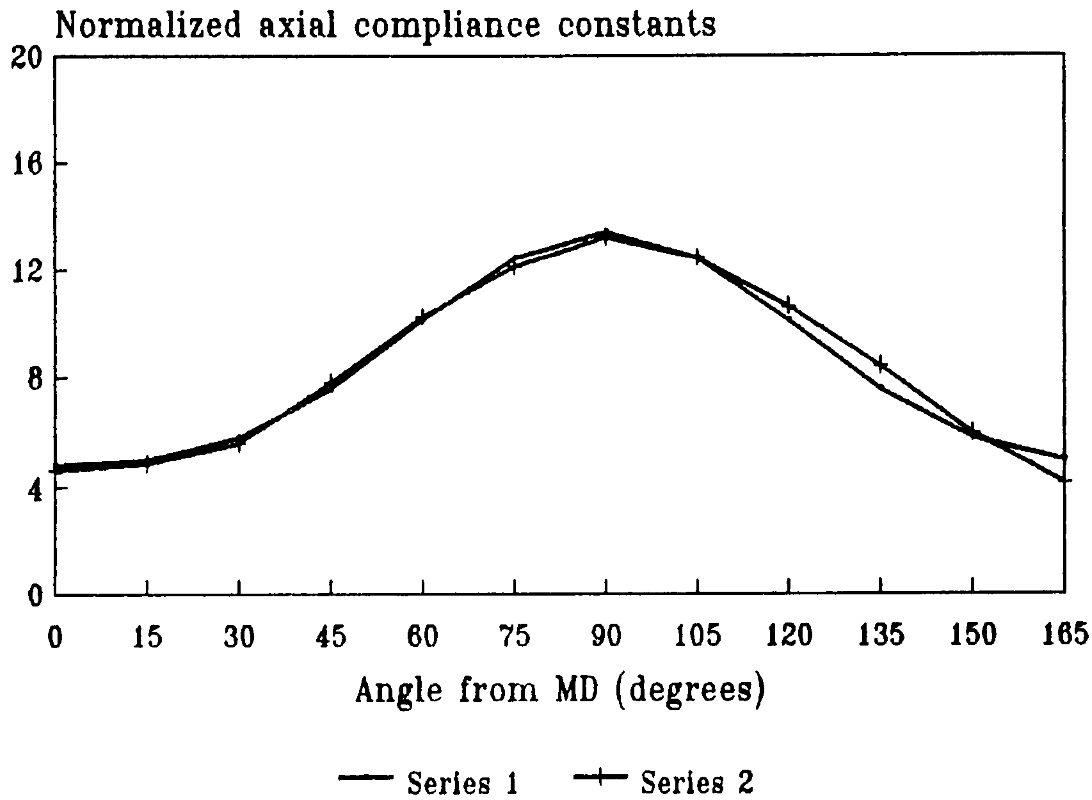

series 1 - from electrical measurements
series 2 - from tensile measurements

Fig. 6.4 Comparison of normalized axial compliance constants of medium-oriented web.

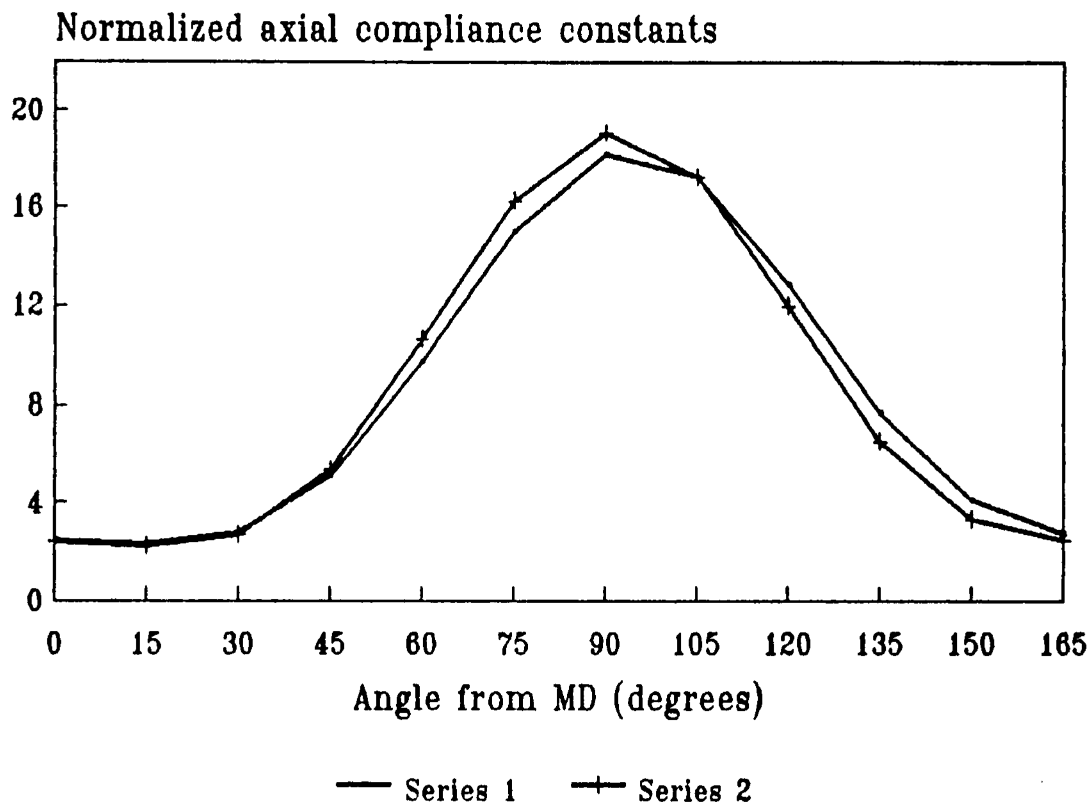

series 1 - from electrical measurements
series 2 - from fiber counting

Fig. 6.5 Comparison of normalized axial compliance constants of highly-oriented web.

0%, (13.4 - 13.2) / 13.4 = 1.5% and (19.0 - 18.0) / 19.0 = 5.3% for the low, medium and highly-oriented webs, respectively.

It was noted in Section 3.1 that the number of stiffness or compliance constants totaled six for the general anisotropic thin web case. Tables 6.5-6.10 show values of all five non-dimensional stiffness (C12 = C66) and all six non-dimensional compliance constants for low-, medium- and highly-oriented webs in 15-degree direction intervals computed from fiber web theory using fiber orientation distributions in Table 6.1. As mentioned in section 3.1, web coupling constants are extremely difficult or impossible to measure experimentally. Tables 6.5-6.10 show that the coupling constants (S16, C16, S26 and C26) exhibit values which are usually zero or small in the principal directions. Thus, although these constants are nearly impossible to obtain experimentally, they are easily computed from the fiber orientation distribution using fiber-web theory. Other inconveniently measured quantities such as the shear modulus and Poisson's ratio also are easily computed as shown in these tables.

Elastic constants in each 15^0 direction in Tables 6.5-6.10 were obtained from fiber-web theory simply by rotating the coordinate axes. Alternatively, constants in other directions may be computed using the transformation equation

Table 6.5 Non-dimensional compliance constants* of low oriented web computed from fiber-web theory using the fiber orientation distribution obtained from electrical measurements.

Angle from M/D (degrees)	S11	S22	S12	S16	S26	S66
0	2.62	3.53	-1.02	0.00	0.00	8.00
15	2.67	3.46	-1.01	0.19	0.27	8.05
30	2.81	3.27	-0.99	0.35	0.44	8.15
45	3.03	3.03	-0.98	0.46	0.46	8.20
60	3.27	2.81	-0.99	0.44	0.35	8.15
75	3.46	2.67	-1.01	0.27	0.19	8.05
90	3.53	2.62	-1.02	0.00	0.00	8.00
105	3.46	2.67	-1.01	-0.27	-0.19	8.05
120	3.27	2.81	-0.99	-0.44	-0.35	8.15
135	3.03	3.03	-0.98	-0.46	-0.46	8.20
150	2.81	3.27	-0.99	-0.35	-0.44	8.15
165	2.67	3.46	-1.01	-0.19	-0.27	8.05

* Compliance constants are obtained from the values in the table divided by E_f.

Table 6.6 Non-dimensional stiffness constants* of low-oriented web computed from fiber-web theory using the fiber orientation distribution obtained from electrical measurements.

Angle from M/D (degrees)	C11	C12	C22	C16	C26
0	0.43	0.12	0.39	0.00	0.00
15	0.42	0.12	0.33	-.14E-1	-.14E-1
30	0.40	0.13	0.35	-.24E-1	-.24E-1
45	0.37	0.13	0.37	-.28E-1	-.28E-1
60	0.35	0.13	0.40	-.24E-1	-2.4E-1
75	0.33	0.12	0.42	-.14E-1	-.14E-1
90	0.32	0.12	0.43	0.00	0.00
105	0.33	0.12	0.42	0.14E-1	0.14E-1
120	0.35	0.13	0.40	0.24E-1	0.24E-1
135	0.37	0.13	0.37	0.28E-1	0.28E-1
150	0.40	0.13	0.35	0.24E-1	0.24E-1
165	0.42	0.12	0.33	0.14E-1	0.14E-1

* Stiffness constants are obtained from the values in the table multiplied by E_f.

Table 6.7 Non-dimensional compliance constants* of medium-oriented web computed from fiber-web theory using the fiber orientation distribution obtained from electrical measurements.

Angle from M/D (degrees)	S11	S22	S12	S16	S26	S66
0	2.12	5.92	-1.35	0.00	0.00	7.97
15	2.20	5.49	-1.17	0.35	1.54	8.66
30	2.55	4.45	-0.83	1.05	2.24	10.04
45	3.33	3.33	-0.66	1.90	1.90	10.73
60	4.45	2.55	-0.83	2.24	1.05	10.04
75	5.49	2.20	-1.17	1.55	0.35	8.66
90	5.92	2.12	-1.35	0.00	0.00	7.97
105	5.49	2.20	-1.17	-1.55	-0.35	8.66
120	4.45	2.55	-0.83	-2.24	-1.05	10.04
135	3.33	3.33	-0.66	-1.90	-1.90	10.73
150	2.55	4.45	-0.83	-1.05	-2.24	10.04
165	2.20	5.49	-1.17	-0.35	-1.54	8.66

* Compliance constants are obtained from the values in the table divided by E_f.

Table 6.8 Non-dimensional stiffness constants* of medium-oriented web computed from fiber-web theory using the fiber orientation distribution obtained from electrical measurements.

Angle from M/D (degrees)	C11	C12	C22	C16	C26
0	0.55	0.13	0.20	0.00	0.00
15	0.53	0.13	0.22	-.44E-1	-.45E-1
30	0.46	0.12	0.29	-.76E-1	-.77E-1
45	0.38	0.12	0.38	-.89E-1	-.89E-1
60	0.29	0.12	0.46	-.77E-1	-.76E-1
75	0.22	0.13	0.53	-.45E-1	-.44E-1
90	0.20	0.13	0.55	0.00	0.00
105	0.22	0.13	0.53	0.45E-1	0.44E-1
120	0.29	0.12	0.46	0.77E-1	0.76E-1
135	0.38	0.12	0.38	0.89E-1	0.89E-1
150	0.46	0.12	0.29	0.76E-1	0.77E-1
165	0.53	0.13	0.22	0.44E-1	0.45E-1

* Stiffness constants are obtained from the values in the table multiplied by E_f.

Table 6.9 Non-dimensional compliance constants* of highly-oriented web computed from fiber-web theory using the fiber orientation distribution obtained from electrical measurements.

Angle from M/D (degrees)	S11	S22	S12	S16	S26	S66
0	1.94	14.34	-2.45	-0.18	-2.20	8.78
15	1.85	13.60	-2.04	0.05	4.51	10.44
30	2.20	10.15	-0.49	1.76	8.16	16.64
45	4.02	6.06	0.65	5.36	7.02	21.18
60	7.67	3.24	0.23	8.14	3.62	19.53
75	11.86	2.15	-1.31	7.08	1.27	13.33
90	14.34	1.94	-2.45	1.85	0.63	8.78
105	13.60	1.85	-2.04	-4.49	0.02	10.44
120	10.15	2.20	-0.49	-7.96	-2.09	16.64
135	6.06	4.02	0.65	-7.03	-5.48	21.18
150	3.24	7.67	0.23	-3.61	-8.15	19.53
165	2.15	11.86	-1.32	-0.88	-7.37	13.33

* Compliance constants are obtained from the values in the table divided by E_f.

Table 6.10 Non-dimensional stiffness constants* of highly-oriented web computed from fiber-web theory using the fiber orientation distribution obtained from electrical measurements.

Angle from M/D (degrees)	C11	C12	C22	C16	C26
0	0.67	0.12	0.93	0.39E-1	0.22E-1
15	0.66	0.12	0.11	-0.46E-1	-0.48E-1
30	0.58	0.12	0.18	-0.12	-0.10
45	0.43	0.13	0.31	-0.15	-0.15
60	0.27	0.14	0.46	-0.14	-0.14
75	0.15	0.13	0.59	-.89E-1	-0.11
90	0.09	0.12	0.67	-.22E-1	-.39E-1
105	0.11	0.11	0.66	0.45E-1	0.46E-1
120	0.18	0.12	0.58	0.10	0.12
135	0.31	0.13	0.43	0.14	0.15
150	0.46	0.14	0.27	0.14	0.14
165	0.59	0.13	0.15	0.11	0.89E-1

* Stiffness constants are obtained from the values in the table multiplied by E_f.

discussed in Section 3.1. Although the transformation equation consists of 81 terms for general anisotropic materials, it can be simplified for two-dimensional orthotropic materials for stiffness constants as follows:

$$
\begin{aligned}
C'_{11} &= C_{11}m^4 + 2\,(C_{12} + 2C_{66})\,m^2n^2 + C_{22}n^4 \\
C'_{22} &= C_{11}n^4 + 2\,(C_{12} + 2C_{66})\,m^2n^2 + C_{22}m^4 \\
C'_{66} &= (C_{11} + C_{22} - 2C_{12} - 2C_{66})\,m^2n^2 + C_{66}(m^4 + n^4) \\
C'_{12} &= (C_{11} + C_{22} - 4C_{66})\,m^2n^2 + C_{12}(n^4 + m^4) \\
C'_{16} &= (C_{11} - C_{12} - 2C_{66})\,m^3n + (C_{12} + 2C_{66} - C_{22})\,mn^3 \\
C'_{26} &= (C_{11} - C_{12} - 2C_{66})\,mn^3 + (C_{12} + 2C_{66} - C_{22})\,m^3n
\end{aligned}
\tag{6.1}
$$

and for compliance constants:

$$
\begin{aligned}
S'_{11} &= S_{11}m^4 + (2S_{12} + S_{66})\,m^2n^2 + S_{22}n^4 \\
S'_{22} &= S_{11}n^4 + (2S_{12} + S_{66})\,m^2n^2 + S_{22}m^4 \\
S'_{12} &= (S_{11} + S_{22} - S_{66})\,m^2n^2 + S_{12}(n^4 + m^4) \\
S'_{16} &= -2\,(S_{11}m^2 - S_{22}n^2)\,nm + (2S_{12} + S_{66})\,nm\,(m^2 - n^2) \\
S'_{26} &= -2\,(S_{11}n^2 - S_{22}m^2)\,nm - (2S_{12} + S_{66})\,nm\,(m^2 - n^2)
\end{aligned}
\tag{6.2}
$$

$$S'_{66} = 4(S_{11} + S_{22} - 2S_{12})m^2n^2 + s_{66}(m^2 - n^2)^2$$

where m = cosθ and n = sinθ. To test the validity of the computed elastic constants, the transformation equations S11' and C11' were computed in every 15^0 direction using the constants in the principal directions for the low- and medium-oriented webs which were assumed to be orthotropic. When compared to values of the constants in Tables 6.5-6.8 obtained by rotating the coordinate axis 15^0 using fiber-web theory, an exact agreement was found.

Elastic constants of the highly oriented web were computed using the fiber orientation distribution obtained from counting fibers under a microscope by rotating the coordinate axis 15^0 using fiber-web theory. Compliance constants and stiffness computed in this manner are shown in Tables 6.11 and 6.12, respectively. When these constants are compared to constants computed from electrical measurements (Tables 6.9-6.10), good agreement can be seen.

Figure 6.6 shows the two curves in figure 6.5 plotted again. Good agreement is seen between normalized axial compliance constants computed from electrical measurements using the theory described in Chapter 3 and computed from fiber counting for the highly-oriented web. A third curve also is plotted in Figure 6.6. This represents compliance constants computed from the electrical measurements without applying the theory developed in Section 4. This curve

Table 6.11 Non-dimensional compliance constants* of highly-oriented web computed from fiber-web theory using fiber orientation distribution obtained from counting fibers under microscope.

Angle from M/D (degrees)	S11	S22	S12	S16	S26	S66
0	2.08	16.36	-3.05	-0.12	-1.14	8.09
15	1.92	14.78	-2.18	-0.23	6.40	11.57
30	2.30	10.29	-0.12	2.19	9.74	19.79
45	4.62	5.60	1.06	6.77	7.47	24.54
60	9.12	2.83	0.19	9.80	2.94	21.06
75	13.97	2.10	-1.86	7.74	0.39	12.84
90	16.36	2.08	-3.05	0.86	0.48	8.09
105	14.78	1.92	-2.18	-6.52	0.40	11.57
120	10.29	2.30	-0.12	-9.68	-2.30	19.79
135	5.60	4.62	1.06	-7.50	-6.82	24.54
150	2.83	9.12	0.19	-3.05	-9.76	21.06
165	2.10	13.97	-1.86	-0.25	-7.85	12.84

* Compliance constants are obtained from the values in the table divided by Ef.

Table 6.12 Non-dimensional stiffness constants* of highly-oriented web computed from fiber-web theory using fiber orientation distribution obtained from counting fibers under microscope.

Angle from M/D (degrees)	C11	C12	C22	C16	C26
0	0.66	0.13	0.09	0.23E-1	0.11E-1
15	0.65	0.12	0.11	-.54E-1	-.61E-1
30	0.56	0.12	0.21	-0.12	-0.11
45	0.41	0.12	0.34	-0.15	-0.14
60	0.25	0.13	0.48	-0.14	-0.13
75	0.14	0.13	0.60	-.84E-1	-.90E-1
90	0.09	0.13	0.66	-.11E-1	-.23E-1
105	0.11	0.12	0.65	0.61E-1	0.54E-1
120	0.21	0.12	0.56	0.11	0.12
135	0.34	0.12	0.41	0.14	0.15
150	0.48	0.13	0.25	0.13	0.14
165	0.60	0.13	0.14	0.90E-1	0.84E-1

* Stiffness constants are obtained from the values in the table multiplied by E_f.

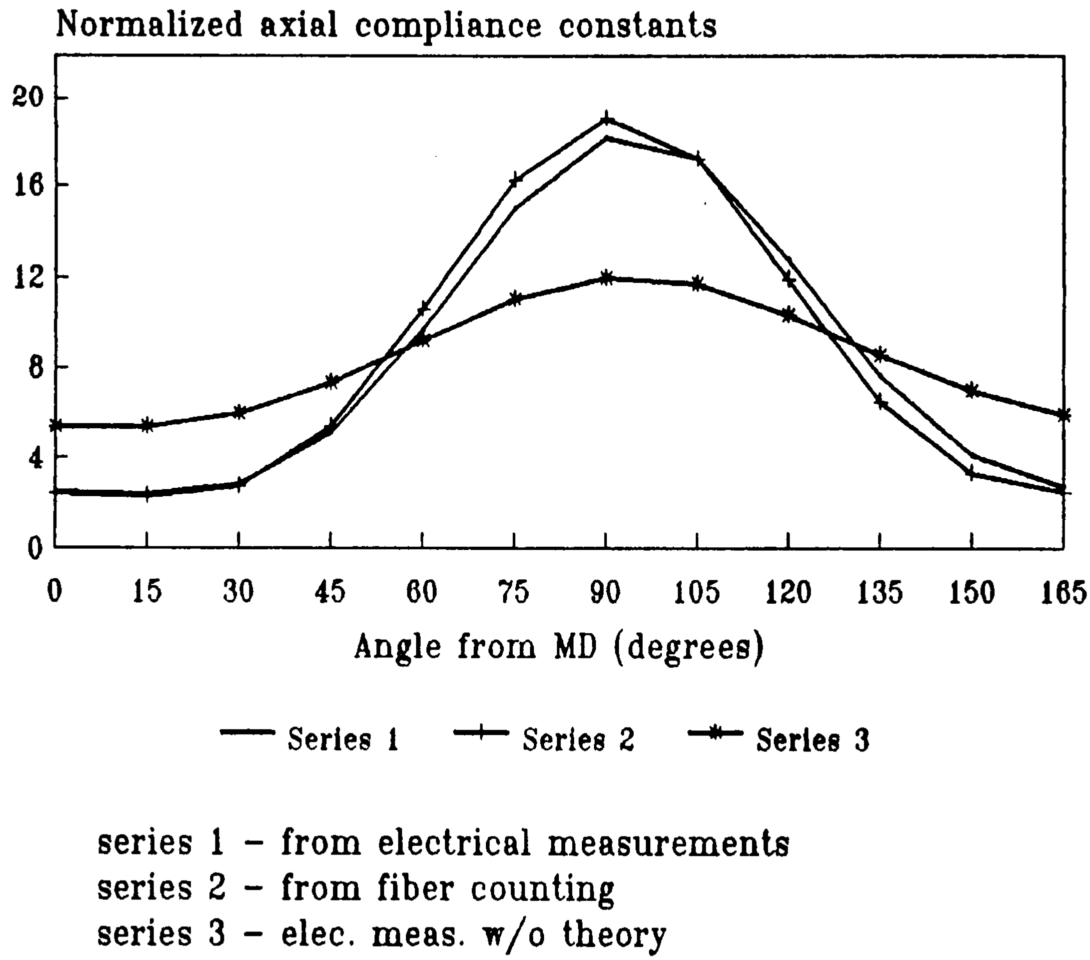

Fig. 6.6 Comparison of normalized axial compliance constants of highly-oriented web.

agrees poorly with compliance constants from the other two curves. This demonstrates that the distribution of electric current does not correlate well with mechanical properties. Instead, a theoretical interpretation of electric currents is necessary. It also suggests why many of the techniques discussed in Chapter 2 were neither adequate nor accurate since no proper theory was developed to relate the fiber orientation distribution to their measurements.

The mechanical behavior of the three webs can be compared conveniently in Figure 6.7 where compliance constants computed from electrical measurements are plotted for each web. The low oriented web can be seen to be nearly isotropic whereas mechanical anisotropy increases with increasing fiber orientation. As was shown previously, these curves agree well with tensile measurements and fiber counting.

The measurement device and theory developed in this Dissertation seem to provide a valid means to determine the fiber orientation distribution and obtain mechanical constants which may be difficult or impossible to measure directly. Although the validity of the method is proved, one may question its convenience. As mentioned in Chapter 5, temperature and relative humidity influence the resistance of the dielectric materials. This was illustrated in Figure 6.1 where different temperature and humidity conditions

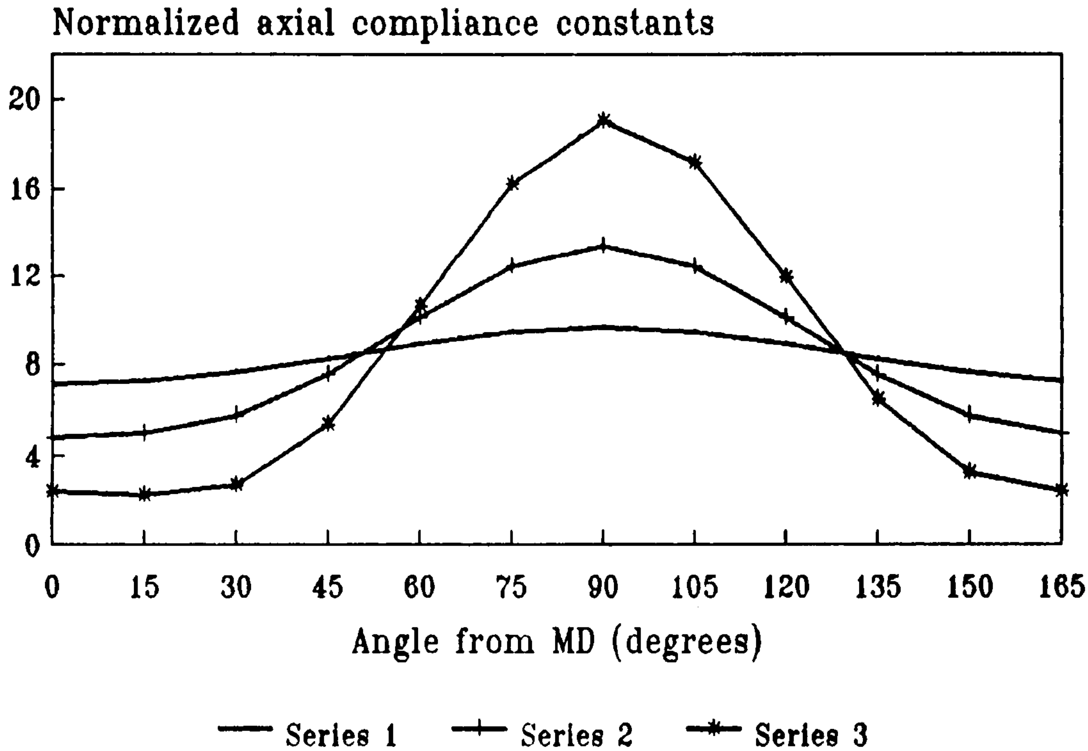

series 1 - low-oriented web
series 2 - medium-oriented web
series 3 - highly-oriented web

Fig. 6.7 Compliance constants of three webs based on electrical measurements.

yielded different current measurement and you may ask what conditions can be used to determine the fiber orientation distribution. Figure 6.2 shows, however, that different currents from different conditions exhibit the same current distribution. Since the first step involved in converting measured currents to the fiber orientation distribution is to normalize the currents to obtain a current distribution, the current unit is eliminated. Therefore, currents measured from any temperature and humidity conditions can be used to compute the fiber orientation distribution as long as equilibrium conditions are achieved.

CHAPTER 7

CONCLUSIONS AND COMMENTS

The fiber orientation distribution in nonwoven webs is an important structural parameter which largely determines mechanical properties of webs. A theory was developed to obtain the fiber orientation distribution in thin webs from electrical measurements. An instrument also was developed to provide appropriate measurements of electrical conductivity through typical high resistance webs. From one set of electrical measurements, a complete set of mechanical constants can be computed in any web direction by either rotating the coordinate axes or by using transformation equations.

The fiber orientation distribution was determined from electrical measurements for three thin webs. When compared to the actual distribution determined by optical microscopy, excellent agreement was observed between the actual fiber distribution and the fiber distribution computed from electrical measurements using the theory developed. On the other hand, poor agreement was observed between the actual fiber distribution and the distribution of electric current without applying the theory.

Axial compliance constants were computed from the fiber distributions determined from electrical measurements. These constants were compared to compliance constants obtained from actual tensile measurements from the webs and excellent agreement was observed.

LIST OF REFERENCES

1. Wadsworth, L.C. and Jones, A.M. "Novel Melt Blown Research Findings," Nonwovens Industry, 44-51, November 1986.

2. Choi, K.J., Spruiell, J.E., Fellers, J.F. and Wadsworth, L.C. "Strength Properties of Melt Blown Nonwoven Webs," Polymer Engineering and Science, Vol. 28, 81-89, Jan. 1988.

3. Backer, S. and Patterson, D.R. "Some Principles of Nonwoven Fabrics," Textile Research Journal, vol. 30, 704-711, 1960.

4. Cox, H.L. "The Elasticity and Strength of Papers and Other Fibrous Materials," British Journal of Applied Physics, Vol. 3, 72-79, 1952.

5. Elmer H. Fleischman, Jr., Ph.D. Thesis, Lawrence University, Appleton, Wisconsin, June 1981.

6. Crosby, C.M., Eusufzai, A. R. K., Mark, R.E., Perkins, R.W., Chang, J.S. and Uplekar, N.V. "A Digitizing System for Quantitative Measurement of Structural Parameters in Paper," Tappi, Vol. 64, No. 3, 103- 106, 1981.

7. Orchard, G.A.J. "The Measurement of Fiber Orientation in Card Webs," J. Text. Inst., T380-T385, 1953.

8. Boulay, R., Drouin, B., Gagnon, R., Bélanger, P.A. and Bernard, P. "Optical Polarizing Effect of Paper at Submillimetre Wavelengths." Far-infrared Science and Technology, SPIE Vol.666, 200-205, 1986.

9. Boulay, R., Drouin, B., Gagnon, R. and Bernard, P. "Paper Fibre Orientation Measurement with a Submillimeter Laser," Journal of Pulp and Paper Science, Vol. 12, No. 1, J26-J29 January 1986.

10. Boulay, R. Drouin, B. and Gagnon, R. "Measurement of Local Fibre Orientation Variations," Journal of Pulp and Paper Science, Vol. 12, No. 6, J177-J181, November 1986.

11. Kallmes, O.J. "Technique for Determining the Fiber Orientation Distribution throughout the Thickness of a Sheet," Tappi, Vol. 52, No. 3, 482-485, March 1969.

12. Prud'homme, R.E., Hien, N.V., Noah, J. and Marchessault, R.H. "Determination of Fiber Orientation of Cellulosic Samples by X-ray Diffraction," Journal of Applied Polymer Science, Vol. 19, 2609-2620, 1975.

13. Rudström, L. and Sjölin, U. "A Method for Determining Fiber Orientation in Paper by Using Laser Light," Svensk Papperstidn, 117-121, March 1970.

14. Goodman, J.W. Introduction to Fourier Optics, McGraw-Hill, San Francisco, 1968.

15. Baum, G.A., Bornhoeft, L.R. "Estimating Poisson Ratios in Paper Using Ultrasonic Techniques," Tappi, Vol. 62, No. 5, 87-90, May 1979.

16 Love, A.E.H. A Treatise on the Mathematical Theory of Elasticity, Dover Publications, New York, 1927.

17. Timoshenko, S.P. and Goodier, J.N. Theory of Elasticity, McGraw-Hill Book Company, New York, 1934.

18. Sokolnikoff, I.S. Mathematical Theory of Elasticity, Robert E. Krieger Publishing Co. Inc. Florida, 1946.

19. Lekhnitskii, S.G. Theory of Elasticity of an Anisotropic Elastic Body, Holden-Day, Inc.

20. Hearmon, R.F.S. An Introduction to Applied Anisotropic Elasticity, Oxford University Press, 1961.

21. Ohanian, H.C. Physics, W.W. Norton & Company, New York, 1985.

22. Neff, Jr., H.P. Basic Electromagnetic Fields, Harper & Row, Publishers, New York, 1987.

23. Balanis, C.A. Advanced Engineering Electromagnetics, John Wiley & Sons, New York, 1989.

24. Lawson, C. and Hanson, R. Solving Least Squares Problems, Prentice-Hall, Englewood Cliffs, New Jersey, 1974.

25. Hearle, J.W.S. "The Electrical Resistance of Textile Materials," Journal of the Textile Institute, T117-T198, 1953.

26. Hersh, S.P. and Montgomery, D.J. "Electrical Resistance Measurements on Fibers and Fiber Assemblies," Textile Research Journal, 805-818, 1952.

27. ASTM Test Method E104, "Maintaining Constant Relative Humidity by Means of Aqueous Solutions," Book of ASTM Standards, American Society for Testing and Materials, Philadelphia.

28. Cook, R.D. and Young, W.C. Advanced Mechanics of Materials, Macmillan Publishing Company, New York, 1985.

APPENDIX

```
1 'PROGRAM1: CURRENT ACQUISITION AND CONVERSION TO
   CURRENT DISTRIBUTION
2 '
4 DIM SSUM(10,15),RATIO(10,15),PERDIST(15),NRATWT(10,15),
  WT(15),NRATIO(10,15),NPERDN(15)
5 LPRINT CHR$(27);"h";CHR$(1)
10 LPRINT "TESTING DATE:",DATE$
15 LPRINT CHR$(27);"h";CHR$(0)
16 FOR I = 1 TO 12
17 READ WT(I)
18 NEXT I
20 SAMPLE$="SAMPLE SPECIFICATION:  "
30 PRINT SAMPLE$ : INPUT SPEC$
40 LPRINT SAMPLE$;SPEC$ : LPRINT
50 INPUT "SUPPLY VOLTAGE   " , VOLT
80 DEF SEG = &HC400
90 INITIALIZE% = 0
100 MY.ADDRESS% = 21
110 CONTROLLER% = 0
120 CALL INITIALIZE%(MY.ADDRESS%, CONTROLLER%)
130 SEND% = 9: ENTER% = 21: M617% = 27: RD$ = SPACE$(50)
140 CMD$="F1R5G1T1X"
145 INPUT "NUMBER OF ITERATION ",NUMBER:INPUT "NUMBER
    FOR DUMMY LOOP ",DLOOPNO
147 LPRINT "SUPPLY VOLTAGE:  "; VOLT; "VOLTS" ; "
    # OF DATA:  " ; NUMBER : LPRINT
148 LPRINT "BEGINNING TIME  ";TIME$;
154 FOR K=1 TO 12
155 BEEP:BEEP:BEEP
160 PRINT "CHANGE TO SAMPLE ";K;" NL WHEN READY": INPUT
    NL$
170 FOR I= 1 TO 3
210 SUM=0
220 FOR J=1 TO NUMBER
230 GOSUB 1000
240 SUM=SUM+RD
250 NEXT J
260 GOSUB 2010
261 PRINT
262 NEXT I
270 NEXT K
275 LPRINT "       ENDING TIME  "; TIME$ : LPRINT
280 SUM=0:CMD$="F0R0G1T1X"
290 INPUT "TEMP, NL WHEN READY", NL$
300 GOSUB 3000
310 SUM=0
320 INPUT "RH, NL WHEN READY", NL$
330 GOSUB 3500
```

```
331 LPRINT CHR$(27);"h";CHR$(1)
332 LPRINT "DATA ANALYSIS "
333 LPRINT CHR$(27);"h";CHR$(0)
334 LPRINT "-----------------------------------------------
    -------------------------------------"
335 LPRINT "WEIGHT OF SAMPLES:":LPRINT
336 FOR I= 1 TO 12
337 IF I = 7 THEN LPRINT "   ";
338 LPRINT "#";I;" ";
339 LPRINT USING ".####"; WT(I);
340 LPRINT "    ";
341 NEXT I
342 LPRINT:LPRINT
344 FOR I = 1 TO 3
345 NTEMPER = NRATWT(I,1)
346 TEMPER=SSUM(I,1)
350 FOR P=1 TO 12
360 IF TEMPER > SSUM(I,P) THEN TEMPER=SSUM(I,P)
365 IF NTEMPER > NRATWT(I,P) THEN NTEMPER = NRATWT(I,P)
370 NEXT P
380 FOR Q= 1 TO 12
390 RATIO(I,Q) = SSUM(I,Q) / TEMPER
394 NRATIO(I,Q) = NRATWT(I,Q) / NTEMPER
400 NEXT Q
410 LPRINT "          SAMPLE 1   SAMPLE 2   SAMPLE 3
    SAMPLE 4   SAMPLE 5   SAMPLE 6"
420 A=1:B=6
430 GOSUB 4000
440 LPRINT "          SAMPLE 7   SAMPLE 8   SAMPLE 9
    SAMPLE 10  SAMPLE 11  SAMPLE 12"
450 A=7:B=12
460 GOSUB 4000
463 LPRINT
465 NEXT I
470 TOTR=0 : NTOTR=0
480 FOR I= 1 TO 3
490 FOR Q= 1 TO 12
500 TOTR = TOTR + RATIO(I,Q)
505 NTOTR = NTOTR + NRATIO(I,Q)
510 NEXT Q
520 NEXT I
530 FOR Q= 1 TO 12
540 FOR I = 1 TO 3
550 SUBTOT = SUBTOT + RATIO(I,Q)
555 NSUBTOT = NSUBTOT + NRATIO(I,Q)
560 NEXT I
570 PERDIST(Q) = SUBTOT/TOTR
574 NPERDN(Q) = NSUBTOT / NTOTR
```

```
576 NSUBTOT = 0
580 SUBTOT=0
590 NEXT Q
595 LPRINT "ORIENTATION DISTRIBUTION" :LPRINT
600 FOR I =1 TO 12
605 IF I=7 THEN LPRINT "  ";
610 LPRINT "#";I;" ";
620 LPRINT USING ".####"; PERDIST(I);
625 LPRINT "   ";
630 NEXT I
640 LPRINT
650 FOR I = 1 TO 12
660 IF I = 7 THEN LPRINT "  ";
670 LPRINT "#"; I; " ";
680 LPRINT USING ".####"; NPERDN(I);
690 LPRINT "   ";
700 NEXT I
705 '
710 ' ENTER DATA HERE
720 '
900 END
1000 CALL SEND%(M617%, CMD$, STATUS%)
1010 CALL ENTER%(RD$, LENGTH%, M617%, STATUS%)
1020 RD$ = LEFT$(RD$, LENGTH%)
1030 PRINT RD$
1040 RD=VAL(RD$)
1045 IF RD<0 THEN ZZ=ZZ+1
1050 IF ZZ>2 THEN INPUT "CHECK THE CONNECTION, NL WHEN
     READY",NL$ : J=0 : ZZ=0
1060 FOR Z=1 TO DLOOPNO: NEXT Z
1070 RETURN
2010 AVG=SUM/NUMBER
2030 SSUM(I,K)=AVG
2035 NRATWT(I,K) = AVG / WT(K)
2040 RETURN
3000 FOR J=1 TO NUMBER
3010 GOSUB 1000
3015 RD=RD*95-20
3020 SUM=SUM+RD
3030 NEXT J
3040 TEMP=SUM/NUMBER
3050 LPRINT "TEMPERATURE IS ";TEMP;"C";
3070 RETURN
3500 FOR J=1 TO NUMBER
3510 GOSUB 1000
3515 RD=RD*100-11
3520 SUM=SUM+RD
3530 NEXT J
```

```
3540 RH=SUM/NUMBER
3560 LPRINT "     RELATIVE HUMIDITY IS ";RH;"%"
3570 RETURN
4000 LPRINT "AVERAGE ";
4010 FOR R=A TO B
4020 LPRINT USING "##.####^^^^";SSUM(I,R);
4030 NEXT R
4035 LPRINT
4040 LPRINT "RATIO   ";
4050 FOR S=A TO B
4060 LPRINT USING "####.##    ";RATIO(I,S);
4070 NEXT S
4075 LPRINT
4080 LPRINT "NRATIO  ";
4090 FOR T = A TO B
4100 LPRINT USING "####.##    "; NRATIO(I,T);
4110 NEXT T
4120 LPRINT
4130 RETURN
```

```
900 'PROGRAM2: APPROXIMATE SOLUTIONS
910 '
970 INPUT "dimension of matrix    ", DM
980 PI = 3.141593
990 DIM A(DM,DM+1), PN(DM), NPERDN(DM), PR(DM), M(DM,DM)
1000 FOR I = 1 TO DM
1010 FOR J = 1 TO DM
1020 A(I,J) = (COS(PI/DM*(I-J)))^2
1030 NEXT J
1035 READ A(I,DM+1)
1040 NEXT I
1175 GOSUB 2000
1180 FOR I = 1 TO DM-1
1181 FOR P = I TO DM
1182 IF A(P,I)<>0  THEN 1185
1183 NEXT P
1184 LPRINT "NO UNIQUE SOLUTION" : GOTO 1250
1185 IF P = I THEN 1190
1186 FOR K = I TO DM+1
1187 A1 = A(P,K): A(P,K)=A(I,K): A(I,K)=A1
1188 NEXT K
1190 FOR J = I+1 TO DM
1200 M(J,I) = A(J,I) / A(I,I)
1210 FOR K = I TO DM+1
1220 A(J,K) = A(J,K) - M(J,I) * A(I,K)
1230 NEXT K
1240 NEXT J
1250 NEXT I
1255 GOSUB 2000
1260 PN(DM) = A(DM,DM+1) / A(DM,DM)
1270 FOR I = DM-1 TO 1 STEP -1
1280 FOR J = I+1 TO DM
1290 TOT = TOT + A(I,J) * PN(J)
1300 NEXT J
1310 PN(I) = (A(I,DM+1) - TOT) / A(I,I)
1330 TOT = 0
1340 NEXT I
```

```
1350 FOR I= I TO DM
1360 TOTPN = TOTPN + PN(I)
1370 NEXT I
1372 LPRINT:LPRINT
1375 PRINT TOTPN
1380 FOR I = 1 TO DM
1390 PR(I) = PN(I)/TOTPN
1400 IF I=7 THEN LPRINT
1410 LPRINT PN(I);
1415 PRINT PR(I)
1420 NEXT I
1425 LPRINT:LPRINT:LPRINT:LPRINT:LPRINT:LPRINT:LPRINT
1490 '
1500 ' INPUT DATA HERE
1510 '
1990 END
2000 LPRINT
2010 FOR I = 1 TO DM
2020 FOR J = 1 TO DM+1
2030 LPRINT USING "###.###"; A(I,J);
2040 LPRINT " ";
2050 NEXT J
2060 LPRINT
2070 NEXT I
2080 RETURN
```

```
C
C        PROGRAM3 -- NONNEGATIVE LEAST SQUARES
C
      DIMENSION A(24,12),B(24),X(12),W(12),ZZ(24)
      INTEGER INDEX(12)
      PRINT *, 'ENTER % BY ELEC. MEAS'
      P=3.141593/12
      OPEN (9, FILE='NNLSIN4.DAT', STATUS='OLD')
        DO  I = 1,12
            DO  J = 1,12
              A(I,J) = (COS(P*(I-J)))**2
            END DO
            READ *, B(I)
        END DO
       PRINT *, 'ENTER ESTIMATE VALUE'
        DO 20 I = 13,24
          READ (9,*) (A(I,J), J=1,12)
20        READ *, B(I)
      CLOSE (9)
      CALL NNLS (A,24,24,12,B,X,RNORM,W,ZZ,INDEX,MODE)
        DO I = 1, 12
        PRINT *, X(I)
        END DO
      PRINT *, 'RESIDUAL  ', RNORM
      END

      SUBROUTINE NNLS (A,MDA,M,N,B,X,RNORM,W,ZZ,INDEX,MODE)
      DIMENSION A(MDA,N), B(M), X(N), W(N), ZZ(M)
      INTEGER INDEX(N)
      ZERO=0
      ONE=1
      TWO=2
      FACTOR=0.01
      MODE=1
      IF (M.GT.0 .AND. N.GT.0) GO TO 10
      MODE=2
      RETURN
10    ITER=0
      ITMAX=3*N
        DO 20 I=1,N
        X(I)=ZERO
20      INDEX(I)=I
      IZ2=N
      IZ1=1
      NSETP=0
      NPP1=1
30    CONTINUE
      IF (IZ1.GT.IZ2 .OR. NSETP .GE. M) GO TO 350
```

```
        DO 50 IZ=IZ1,IZ2
        J=INDEX(IZ)
        SM=ZERO
            DO 40 L=NPP1,M
40          SM=SM+A(L,J)*B(L)
50      W(J)=SM
60    WMAX=ZERO
        DO 70 IZ=IZ1,IZ2
        J=INDEX(IZ)
        IF (W(J).LE.WMAX) GO TO 70
        WMAX=W(J)
        IZMAX=IZ
70      CONTINUE
      IF (WMAX) 350,350,80
80    IZ=IZMAX
      J=INDEX(IZ)
      ASAVE=A(NPP1,J)
      CALL H12 (1,NPP1,NPP1+1,M,A(1,J),1,UP,DUMMY,1,1,0)
      UNORM=ZERO
      IF (NSETP.EQ.0) GO TO 100
        DO 90 L=1,NSETP
90    UNORM=UNORM+A(L,J)**2
100   UNORM=SQRT(UNORM)
      IF (DIFF(UNORM+ABS(A(NPP1,J))*FACTOR,UNORM)) 130,
     * 130,110
110   DO 120 L=1,M
120   ZZ(L)=B(L)
      CALL H12 (2,NPP1,NPP1+1,M,A(1,J),1,UP,ZZ,1,1,1)
      ZTEST=ZZ(NPP1)/A(NPP1,J)
      IF (ZTEST) 130,130,140
130   A(NPP1,J)=ASAVE
      W(J)=ZERO
      GO TO 60
140     DO 150 L=1,M
150     B(L)=ZZ(L)
      INDEX(IZ)=INDEX(IZ1)
      INDEX(IZ1)=J
      IZ1=IZ1+1
      NSETP=NPP1
      NPP1=NPP1+1
      IF (IZ1 .GT. IZ2) GO TO 170
        DO 160 JZ=IZ1,IZ2
        JJ=INDEX(JZ)
160     CALL H12 (2,NSETP,NPP1,M,A(1,J),1,UP,A(1,JJ),1,
     *  MDA, 1)
170   CONTINUE
      IF (NSETP.EQ.M) GO TO 190
        DO 180 L=NPP1,M
180     A(L,J)=ZERO
190   CONTINUE
```

```
      W(J)=ZERO
      ASSIGN 200 TO NEXT
      GO TO 400
200   CONTINUE
210   ITER=ITER+1
      IF (ITER.LE.ITMAX) GO TO 220
      MODE=3
      WRITE (6,440)
      GO TO 350
220   CONTINUE
      ALPHA=TWO
        DO 240 IP=1,NSETP
        L=INDEX(IP)
        IF (ZZ(IP)) 230,230,240
230   T=-X(L)/(ZZ(IP)-X(L))
      IF (ALPHA.LE.T) GO TO 240
      ALPHA=T
      JJ=IP
240   CONTINUE
      IF (ALPHA.EQ.TWO) GO TO 330
        DO 250 IP=1,NSETP
        L=INDEX(IP)
250   X(L)=X(L)+ALPHA*(ZZ(IP)-X(L))
      I=INDEX(JJ)
260   X(I)=ZERO
      IF ( JJ.EQ.NSETP) GO TO 290
      JJ=JJ+1
        DO 280 J=JJ,NSETP
        II=INDEX(J)
        INDEX(J-1)=II
        CALL G1 (A(J-1,II),A(J,II),CC,SS,A(J-1,II))
        A(J,II)=ZERO
            DO 270 L=1,N
            IF (L.NE.II) CALL G2 (CC,SS,A(J-1,L),A(J,L))
270         CONTINUE
280     CALL G2 (CC,SS,B(J-1),B(J))
        PRINT*, 'TEST STOP'
290   NPP1=NSETP
      NSETP=NSETP-1
      IZ1=IZ1-1
      INDEX(IZ1)=I
        DO 300 JJ=1,NSETP
        I=INDEX(JJ)
        IF (X(I)) 260,260,300
300   CONTINUE
        DO 310 I=1,M
310   ZZ(I)=B(I)
      ASSIGN 320 TO NEXT
      GO TO 400
320   CONTINUE
```

```
      GO TO  210
330     DO 340 IP=1,NSETP
        I=INDEX(IP)
340     X(I)=ZZ(IP)
      GO TO 30
350   SM=ZERO
      IF (NPP1.GT.M) GO TO 370
        DO 360 I=NPP1,M
360     SM=SM+B(I)**2
      GO TO 390
370     DO 380 J=1,N
380     W(J)=ZERO
390   RNORM=SQRT(SM)
        RETURN
400     DO 430 L=1,NSETP
        IP=NSETP+1-L
        IF (L.EQ.1) GO TO 420
            DO 410 II=1,IP
410         ZZ(II)=ZZ(II)-A(II,JJ)*ZZ(IP+1)
420     JJ=INDEX(IP)
430     ZZ(IP)=ZZ(IP)/A(IP,JJ)
       GO TO NEXT, (200,320)
        PRINT*, 'TEST STOP'
440    FORMAT (35H0 NNLS QUITTING ON ITERATION COUNT.)
       END

        SUBROUTINE H12 (MODE,LPIVOT,L1,M,U,IUE,UP,C,ICE,
      * ICV,NCV)
        DIMENSION U(IUE,M), C(1)
        DOUBLE PRECISION SM,B
        ONE=1
        IF (0.GE.LPIVOT.OR.LPIVOT.GE.L1.OR.L1.GT.M) RETURN
        CL=ABS(U(1,LPIVOT))
        IF (MODE .EQ. 2) GO TO 60

            DO 10 J=L1,M
10          CL=AMAX1(ABS(U(1,J)),CL)
        IF (CL) 130,130,20
20      CLINV=ONE/CL
        SM=(DBLE(U(1,LPIVOT))*CLINV)**2
          DO 30 J=L1,M
30        SM=SM+(DBLE(U(1,J))*CLINV)**2
        SM1=SM
        CL=CL*SQRT(SM1)
        IF (U(1,LPIVOT)) 50,50,40
40      CL=-CL
50      UP=U(1,LPIVOT)-CL
        U(1,LPIVOT)=CL
        GO TO 70
```

```
60        IF (CL) 130,130,70
70        IF (NCV.LE.0) RETURN
          B=DBLE(UP)*U(1,LPIVOT)
          IF (B) 80,130,130
80        B=ONE/B
          I2=1-ICV+ICE*(LPIVOT-1)
          INCR=ICE*(L1-LPIVOT)
            DO 120 J=1,NCV
            I2=I2+ICV
            I3=I2+INCR
            I4=I3
            SM=C(I2)*DBLE(UP)
              DO 90 I=L1,M
              SM=SM+C(I3)*DBLE(U(1,I))
90            I3=I3+ICE
            IF (SM) 100,120,100
100         SM=SM*B
            C(I2)=C(I2)+SM*DBLE(UP)
              DO 110 I=L1,M
              C(I4)=C(I4)+SM*DBLE(U(1,I))
110           I4=I4+ICE
120         CONTINUE
130       RETURN
          END

          SUBROUTINE G1 (A,B,COS,SIN,SIG)
          ZERO=0
          ONE=1
          IF (ABS(A).LE.ABS(B)) GO TO 10
          XR=B/A
          YR=SQRT(ONE+XR**2)
          COS=SIGN(ONE/YR,A)
          SIN=COS*XR
          SIG=ABS(A)*YR
          RETURN
10        IF (B) 20,30,20
20        XR=A/B
          YR=SQRT(ONE+XR**2)
          SIN=SIGN(ONE/YR,B)
          COS=SIN*XR
          SIG=ABS(B)*YR
          RETURN
30        SIG=ZERO
          COS=ZERO
          SIN=ONE
          RETURN
          END
```

```
SUBROUTINE G2 (COS,SIN,X,Y)
XR=COS*X+SIN*Y
Y=-SIN*X+COS*Y
X=XR
RETURN
END
FUNCTION DIFF(X,Y)
DIFF=X-Y
RETURN
END
```

```
1 'PROGRAM-1: CALCULATION OF MODULUS AND COMPLIANCE
   CONSTANTS FROM FIBER ORIENTAION DISTRIBUTION
2 '
5 DIM CURRT(12), PROB(12)
10 FOR I=1 TO 12
20 READ CURRT(I)
30 CURRN=CURRN + CURRT(I)
40 NEXT I
50 FOR J=1 TO 12
60 PROB(J) = CURRT(J)/CURRN
65 LPRINT PROB(J)
70 NEXT J
90 FOR K = 1 TO 12
95 THETA = (K-1)*(3.1415927#/12)
100 ALFA1 = 2 * COS(2*THETA) * PROB(K)
110 ALFA2 = 2 * COS(4*THETA) * PROB(K)
120 BETA1 = 2 * SIN(2*THETA) * PROB(K)
130 BETA2 = 2 * SIN(4*THETA) * PROB(K)
140 SALFA1 = SALFA1 + ALFA1
150 SALFA2 = SALFA2 + ALFA2
160 SBETA1 = SBETA1 + BETA1
170 SBETA2 = SBETA2 + BETA2
180 NEXT K
190 C11 = ( SALFA2 + 4 * SALFA1 + 6 ) / 16
200 C12 = ( 2 - SALFA2 ) / 16
210 C22 = ( SALFA2 - 4 * SALFA1 + 6 ) / 16
220 C16 = ( 2 * SBETA1 + SBETA2 ) / 16
230 C26 = ( 2 * SBETA1 - SBETA2 ) / 16
240 DELTA = (2+SALFA2-SALFA1^2)*(2-SALFA2-SBETA1^2)-
    (SALFA1*SBETA1-SBETA2)^2
250 S11 = ((2-SALFA2)*(6-4*SALFA1+SALFA2)-(2*SBETA1-
    SBETA2)^2)/DELTA
260 S22 = ((2-SALFA2)*(6+4*SALFA1+SALFA2)-(2*SBETA1+
    SBETA2)^2)/DELTA
270 S12 = - ((2-SALFA2)^2-4*SBETA1^2+SBETA2^2)/DELTA
280 S16 = - 4*((2-2*SALFA1+SALFA2)*SBETA1+(2-SALFA1)*
    SBETA2)/ DELTA
290 S26 = - 4*((2+2*SALFA1+SALFA2)*SBETA1-(2+ALFA1)*
    SBETA2)/DELTA
300 S66 = 16 * ( 2 + SALFA2 - SALFA1 ^ 2 ) / DELTA
```

```
305 LPRINT
310 LPRINT " c11=    ", C11
320 LPRINT " c12=    ", C12
330 LPRINT " c22=    ", C22
340 LPRINT " c16=    ", C16
350 LPRINT " c26=    ", C26
360 LPRINT " s11=    ", S11
370 LPRINT " s22=    ", S22
380 LPRINT " s12=    ", S12
390 LPRINT " s16=    ", S16
400 LPRINT " s26=    ", S26
410 LPRINT " s66=    ", S66
415 LPRINT:LPRINT:LPRINT
500 '
510 'ENTER DATA HERE
520 '
```

```
1 'PROGRAM5: CALCULATION OF COMPLIANCE CONSTANTS FROM
  TENSILE TESTING
2 '
10 DIM WT(15), NCOMP(15)
50 INPUT "GAUGE LENGTH  ", GL
60 LPRINT "GAUGE LENGTH  ", GL
100 INPUT "CHART SPEED  ", CS
110 LPRINT "CHART SPEED  ", CS
200 INPUT "X-HEAD SPEED  ", XS
210 LPRINT "X-HEAD SPEED  ", XS
215 LPRINT
250 FOR I = 1 TO 12
300 READ WT(I)
310 LPRINT "WT. OF SAMPLE  "; I, WT(I)
320 SUM = SUM + WT(I)
330 NEXT I
335 LPRINT
340 AVG = SUM / 12
345 LPRINT "AVERAGE OF WT  ", AVG
347 LPRINT:LPRINT
350 FOR I = 1 TO 12
400 READ LLOAD
410 LPRINT "LOAD  "; I , LLOAD
500 READ CE
510 LPRINT "CHART EXTENSION  ", CE
600 TIME = CE / CS
700 CHFL = TIME * XS
800 STRAIN = CHFL / GL
900 COMPL = STRAIN / LLOAD
950 LPRINT "COMPLIANCE  ", COMPL
1000 WTR = WT(I) / AVG
1100 STRESS = LLOAD / WTR
1200 NCOMP(I) = STRAIN / STRESS
1300 SUMNCOM = SUMNCOM + NCOMP(I)
1400 LPRINT "NCOMPLIANCE  ", NCOMP(I)
1450 LPRINT
1500 NEXT I
```

```
1600 FOR I = 1 TO 12
1700 RCOMP = NCOMP(I) / SUMNCOM
1800 LPRINT "RCOMP  ", I, RCOMP
1900 NEXT I
1950 LPRINT:LPRINT
2000 TEMP = NCOMP(1)
2100 FOR I = 1 TO 12
2200 IF TEMP < NCOMP(I) THEN 2400
2300 TEMP = NCOMP(I)
2400 NEXT I
2500 FOR I = 1 TO 12
2600 RATIO = NCOMP(I) / TEMP
2700 LPRINT "RATIO  ", I, RATIO
2800 NEXT I
2900 '
3000 'ENTER DATA IN THE SEQUENCE OF WEIGHT ALONG
     THEN LOAD/CHART LENGTH STARTING HERE
3100 '
5000 END
```

VITA

The author, Peter Ping-yi Tsai, is from Taiwan. His first undergraduate major was Textile Chemistry. After graduation, he worked for four years in the Textile industry and then he came to the United States for further studies. He received his M.S. in Mechanical Engineering Technology and then received a second B.S. in Computer Science. He taught Mathematics for two years as a graduate teaching assistant at Kansas State University. He worked as a graduate research assistant for a total of six years at Pittsburg State University, Kansas State University , and The University of Tennessee, writing computer programs, designing system controls, and studying nonwovens and textiles.